Dream Stream Propulsion System

2023 AIAA Engine Design Competition

Milwaukee School of Engineering

Advisor

Dr. Prabhakar Venkateswaran

Team Lead

Cade Beekman

Team Members

Izaiah Dietrich

Michael Gavin

Devon Lallensack

Davis Mattingly

Signatures

Faculty Advisor
Dr. Prabhakar Venkateswaran

Team Lead
Cade Beekman
Member ID: 1401547

Team Member
Izaiah Dietrich
Member ID: 1401430

Michael Gavin

**Team Member
Michael Gavin
Member ID: 1401548**

Devon Lallensack

**Team Member
Devon Lallensack
Member ID: 1401546**

Mia Mattingly

**Team Member
Mia Mattingly
Member ID: 1401432**

Table of Contents

Table of Tables

Table of Figures

Nomenclature

β – Bypass ratio

f – Fuel air ratio

DoH – Degree of hybridization

HV – fuel heating value

TSFC – Thrust specific fuel consumption

LP – Low Pressure

HP – High Pressure

$\tau_{turbofan}$ – Thrust produced by a single turbofan engine

τ_{BLI} – Thrust produced by the aft fan

η_p – Propulsive efficiency

η_{th} – Thermal efficiency

η_o – Overall efficiency

u – Free stream velocity of the engine

$u_{e,core}$ – Exhaust velocity of the engine core

$u_{e,bypass}$ – Exhaust velocity of the bypass stream

Abstract

This report details the design of a propulsion system for a single-aisle commercial aircraft utilizing boundary layer ingestion as requested by the 2023 AIAA Undergraduate Engine design competition. The proposed Dream Stream Propulsion System is expected to meet thrust requirements and be safely operable over the entire course of a typical flight profile. Boundary layer ingestion is a highly researched topic presently due to the expected benefits in terms of fuel consumption. As a result, the main goal for the design of the Dream Stream Propulsion system was to reduce the fuel burn of the aircraft. With an expected entry date of 2035, upgrades in material technology were considered and were incorporated in the development of the new propulsion system design.

The design of the Dream Stream Propulsion System focused primarily on optimizing the existing baseline engine according to the new material constraints. Due to boundary layer ingestion through an aft fan located at the rear of the fuselage, the goal was to produce the target thrust with smaller turbofan engines, so that the weight of the new propulsion system closely resembled that of the conventional propulsion system including only the two wing-mounted engines.

1. Introduction

A new propulsion system design is required for the NASA STARC-ABL single-aisle commercial aircraft. The current design on this aircraft was proposed in 2016 and incorporated two wing-mounted turbofan engines with an aft-fan at the rear of the fuselage that utilizes boundary layer ingestion [1]. The implementation of boundary layer ingestion technology in aircraft propulsion system shows to be promising due to the significant benefits it can have in terms of fuel consumption. The fuel consumption savings are largely a result of ingesting the lower speed air in the fuselage boundary layer, allowing for more efficient momentum change of the air to produce thrust [2,3].

With an entry-into-service date in 2035, limits to the compressor exit temperature (T3) and the turbine inlet temperature (T4) can be estimated and increased, allowing for further optimization of the baseline CFM56-7B24 engines [1]. Our team put extensive research into estimating these material limits and used this information to select new operating conditions at cruise for the new propulsion system. Temperature selections, pressure ratio selections, bypass ratio, and other important parameters were changed to minimize the TSFC of the propulsion system. Maintaining a safe design was just as crucial over all of the operating conditions was just as important to our team, so the aforementioned parameters and materials were selected to ensure the design was always within specified stress margins, surge margins, while meeting thrust requirements and remaining within the constraints described in the 2023 AIAA Engine Design Competition Request for Proposal (RFP) and enumerated in the following sections.

1.1 Design Constraints
- Design must consist of two conventional turbofan engines carried on pylons beneath the wings with power extracted evenly from both turbofans to drive an electric fan at the rear of the fuselage [1]
- The design is to be made for the NASA STARC-ABL Aircraft [1]
- A burner pressure loss of 4% should be used to ensure complete mixing and efficient combustion [1]
- The power off-take or power extracted to power the aircrafts onboard systems is to be set to 150 hp to ensure enough power for onboard systems (excludes electric fan) [1]
- Design will operate with a turbine entry temperature no greater than 3150 R and a compressor entry temperature no greater than 1620 R [1]
- The turbine and compressor disks must be sized to support a minimum stress margin of at least 15%
- Compressors must operate beyond a 20% surge margin
- The new hybrid electric model should be designed for cruise conditions at 35,000 ft and Mach 0.8 but still meet takeoff requirements at sea level

1.2 Design Objectives

- Investigate and quantify the effects of the DOH on performance and net thrust on the new propulsion model
- Boundary layer ingestion to be studied and quantified to show the optimal range of boundary layer intake and present the attractive benefits for future aerospace technology
- Design to have an overall pressure ratio at maximum power equal to or higher than the current baseline model.
- The net-thrust produced by the hybrid-electric propulsion system at sea-level takeoff to be equal to or greater than the baseline model.
- The specific fuel consumption of the new propulsion system at top of climb cruise conditions to be less than that of the baseline model.

1.3 Design Specifications

The design specifications created by our group were the quantifiable metrics that our designs had to meet for them to be considered viable, even if they met all of the design constraints.

- Turbofan design should not exceed more than a 10% increase in weight compared to the baseline turbofan
- Turbofan design should be no more than 10% longer than the baseline turbofan
- Propulsion system design should improve thrust specific fuel consumption at cruise by a minimum of 7% compared to the baseline model
- Keep the maximum thrust at sea level within 5% of the baseline model

<u>1.4 Key Achievements of the Dream Stream Propulsion System</u>

By following all of the design parameters and carefully considering the different trade studies, the proposed Dream Stream Propulsion System design was able to meet every requirement set by our team and the RFP. Some of these achievements are listed as follows:

- 14% decrease in effective TSFC at cruise

- 43% decrease in turbofan weight

- 24% decrease in weight after considering aft fan

- 4% increase in thermal efficiency

- 6.6% increase in propulsive efficiency

- Design is viable for all surge and stress margin specifications

In the following sections of the report, the methods our team used to get to these results are described in detail.

2. Background and Engine Architectures

Background information and current state-of-the-art designs were researched to provide our group with direction towards initial design concepts. Performance parameters were developed and analyzed to define the strength of the

engine designs respective to the baseline. Using research on the different engine architectures and state-of-the-art designs, our team was able to rule out certain designs that were not practical for this application.

2.1 Performance Parameters

An important part in the design of an aircraft engine is to define and utilize parameters to quantify and compare performance. One of the most important performance parameters for aircraft engines is the thrust specific fuel consumption (TSFC) and is shown in Eq (1).

$$TSFC = \frac{\dot{m}_f}{\tau} \tag{1}$$

This metric is defined by the mass flow rate of fuel normalized by the thrust produced [4]. However, for the purposes of the AIAA Engine Design Competition, this performance parameter must be defined more clearly. Thrust specific fuel consumption could be a misleading parameter for a hybrid-electric propulsion system because on a conventional propulsion system, this only includes the thrust of the turbofan in calculations. A hybrid-electric propulsion system extracts more power from the turbofan engine to power and electric fan that produces thrust, which when only considering the turbofan engine in the thrust specific fuel consumption, disadvantages hybrid-electric propulsion systems [2]. Therefore, it is important to note that in order to create valid comparisons between the two propulsion systems, the total mass flow rate of the fuel, and the total thrust produced by the entire propulsion system should be accounted for. For this, our group produced an effective TSFC parameter to account for the thrust produced by the aft fan. This is shown in Eq (2).

$$Effective\ TSFC = TSFC * \frac{2*\tau_{turbofan}}{2*\tau_{turbofan}+\tau_{BLI}} \tag{2}$$

There are also a series of thermodynamically defined efficiencies that can be used to characterize the performance of an engine. One of these is a parameter called the propulsive efficiency which is shown in Eq (3).

$$\eta_P = \frac{2u\tau}{\dot{m}_{a,core}[(1+f)u_{e,core}^2+\beta u_{e,bypass}^2-(1+\beta)u^2]} \tag{3}$$

This efficiency is a measure of how well the kinetic energy of the flow is converted into propulsive power. Another efficiency that is defined is the thermal efficiency of the turbofan engine, which is shown in Eq (4).

$$\eta_{th} = \frac{[(1+f)u_{e,core}^2 + \beta u_{e,bypass}^2 - (1+\beta)u^2]}{2fHV} \tag{4}$$

This term is often used to characterize the efficiency in all types of thermodynamic cycles and is essentially a ratio of how much chemical energy was converted into kinetic energy. The product of the previous two efficiencies is the overall efficiency and represents the conversion of chemical energy to propulsive power as seen in Eq (5) [4]. The range of the aircraft is directly proportional to the overall efficiency as shown by the Breguet range equation [6].

$$\eta_O = \eta_P \eta_{th} \tag{5}$$

A parameter that has risen with the advent of hybrid-electric propulsion systems is the degree of hybridization (DoH). This parameter aims to define the amount of power that can be extracted to power the electric fan from any particular spool on a turbofan engine and is shown in Eq (6).

$$DoH = \frac{Power\ Extraction}{Power\ Extraction + \tau u} \tag{6}$$

For current turbofan engines without a large amount of power extraction, the value of this parameter is essentially zero because power is only extracted to power the on board systems. It is found by taking the ratio of the amount of power extracted to the sum of that same value with the thrust power [1]. Through the use of these performance parameters, the turbofan engine design, and propulsive system as a whole can be characterized and compared quantitatively.

2.2 Engine Architecture

Although a constraint of the 2023 Engine Design Competition is that the presented engine must be a turbofan, it is important to recognize why this is the best available option for the application. Propeller engines are often used for

flight Mach numbers, M, up to 0.6. Turbofan engines are often used to bridge the gap between 0.6 M and sonic conditions, and turbojet engines are used for supersonic cases [6]. The ranges mentioned previously are only general guidelines, as specific situations like fighter jets can implement a low-bypass turbofan engine for supersonic flight that requires frequent direction change. The design competition calls for the propulsion system to be designed for a single-aisle commercial aircraft operating at top-of-climb conditions of 0.8 M [2]. Turbofan engines are also much quieter at high subsonic Mach numbers compared to propellors and turbojets, which makes them especially beneficial for commercial travel. There are also mixed and unmixed turbofans. A mixed turbofan combines the bypass and exhaust flow and is beneficial for limiting noise production, whereas an unmixed turbofan does not do this but weighs less [6].

One of the ways a turbofan's performance can be increased is by making it a geared turbofan. A geared turbofan incorporates a gearbox coupling the inlet fan of the turbofan to the turbine stage it is connected to. The gear ratio employed allows the fan and turbine to spin at different speeds, which is beneficial because the ideal fan and turbine rotational speeds likely differ. This also helps provide better control over the blade tip speed of the fan so that the relative flow at the tip can remain subsonic. This allows for higher bypass ratios to be achieved which is important for the system efficiency, as well as reducing the operating noise levels [7]. However, due to the extra weight and maintenance complexity of this component, most commercial aircraft engines do not currently employ this technology.

Another existing technology that can be implemented is adding a third spool to the turbofan engine. The third spool adds a third concentric shaft to the engine, and implements low, intermediate, and high-pressure stages. Some benefits of adding a third spool include a reduced likelihood of stalling, better turbine efficiency, easier start-up, and better speed matching for the connected components [8,10]. For example, there is a conceptual design that improves upon the baseline 2010 EIS engine [9]. This design claims to be optimized through the use of a 3-shaft turbofan engine and would result in a fuel consumption savings of 11%. Their optimization had a 2.2% increase in the length of the engine, and a fan diameter increase of 22% [9]. It can be inferred that much of the fuel savings from the conceptual engine design mentioned previously can be mainly attributed to the increase in the fan diameter, as well to the additional spool. Increasing the fan diameter is going to increase the bypass ratio, which is a big contributor to

lowering specific fuel consumption [6]. An obvious downfall of implementing a third spool is that it can add significant weight and complexity. This brings forth another type of spool that was researched which was a dual-drive booster spool. In this design an epicyclic gearbox connects the low-pressure spool, high pressure spool, and the booster spool. The epicyclic gearbox acts as a summation gearbox which extracts power from both engine spools in order to power the booster spool. This booster spool could provide great control over the power extraction aspect in the engine [11]. An example of this spool is depicted in Figure 1.
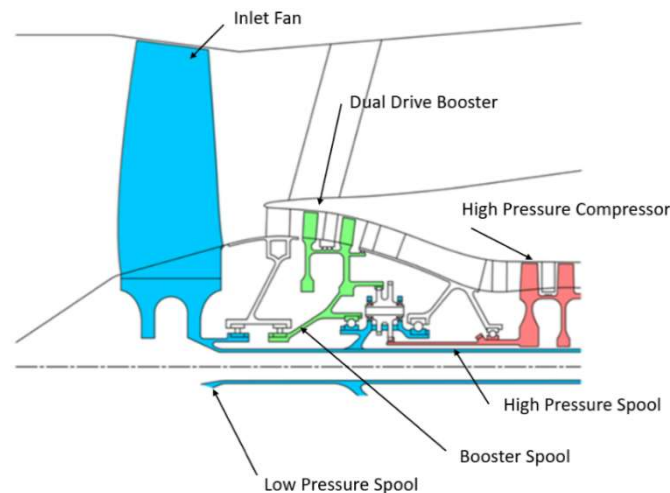
Figure 1: Dual drive booster spool schematic [11]

It is widely known that high bypass ratios result in decreased specific fuel consumption for a turbofan engine. The reason this is attractive is because thrust is related to the product of the air mass flow and its change in velocity, so increasing the fan diameter will allow much larger mass flow rates to experience the change in velocity, resulting in higher thrust values. This in result is more efficient because it will take less power to change the velocity of the lower speed boundary layer air, than it would be to put more power into changing the velocity by a greater amount for the faster free-stream air. Some physical constraints exist, such as engine clearance to the ground on takeoff and increased drag penalties, that limit how high the bypass ratio can get. Improving the upper limit of bypass ratios for turbofan engines is a constant area of research. Further challenges include the fact that the weight and drag increase with the size of inlet fan, which needs to get bigger as the bypass ratio is increased. One of the emerging technologies that is being researched is that of the ultra-high bypass ratio turbofan engine. Ultra-high bypass ratios

can be considered as turbofan engines that have bypass ratios of higher than 10 and upwards of 20. The commercial aircraft engine industry has evolved from low bypass ratios of around 2, to bypass ratios that can reach upwards of 12. Therefore, it only makes sense that this ratio will continue to increase over time. These engines are considered the best option for the future of aircraft propulsion and can have an estimated 25% increase in efficiency, as well as potential noise reduction [11].

3. Propulsion System Preliminary Design Process

The design process for the Dream Stream Propulsion System was centered around the constraints, objectives, and specifications described in section 1 of this report. Our team wanted to keep the engine similar to the baseline so that the weight and length of the engine could remain similar to the baseline. Ultimately, the recreation of the baseline model was an essential aspect in determining the target goals for the new propulsion system design.

3.1 Baseline Engine Model

The baseline engine model for the NASA STARC-ABL is the CFM56-7B24 engine. This is also the engine model architecture that is used for planes like the Boeing 737 and other single-aisle commercial aircraft. The team's recreation of the baseline engine model was an important first step in the Dream Stream Propulsion System design process because it would yield the target values for the new design. It also served as a tool to give the team experience in GasTurb14, which is the software used to do the design calculations in this project.

The values reported for the baseline model relate to takeoff, or static sea-level conditions. The reported values included thrust, TSFC, and dry weight, and these values served as metrics for properly recreating the baseline. The GasTurb14 software provides the ability to do both a thermodynamic, and basic geometry analysis. More importantly, the software allows the engine to be run off of its design point. Once the on-design calculations were performed for takeoff, the off-design calculations were run at cruise conditions. The generic cross section of an unmixed turbofan is shown in Figure 2, and it is labeled with all of the necessary station numbers.
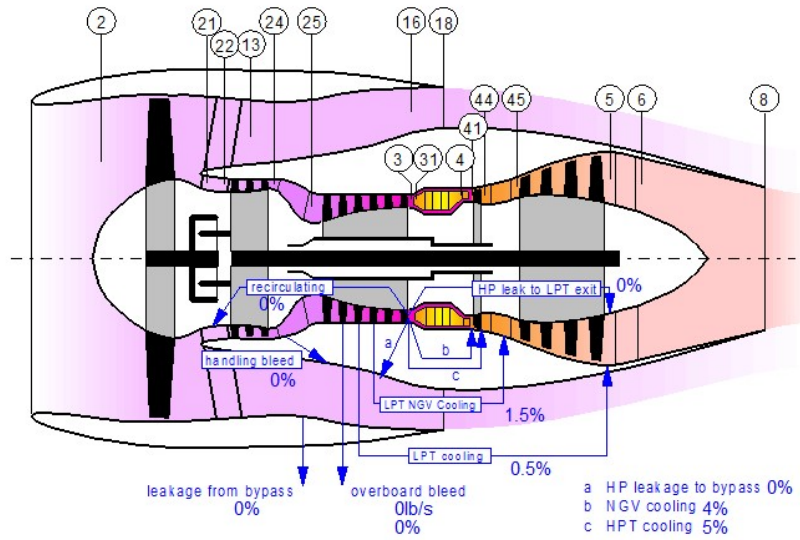
Figure 2: Generic cross section of an unmixed turbofan with station numbers in GasTurb14

In creating the baseline model, our team first looked at matching thermodynamic performance of the engine. Through the process of adjusting mass flows, temperatures, pressure ratios, and efficiencies among other properties, the thermodynamic state at each component can be solved for. Our team has also developed MATLAB functions for each component of the engine, that are able to verify the results obtained from GasTurb14, at least thermodynamically. The results from this first pass recreation of the CFM56-7B24 engine are shown in Table 1.

Table 1: Thermodynamic results from the recreation of the CFM56-7B24 engine model in GasTurb14 [1]

	RFP	Recreated Model	Comparison
Cruise Thrust (lbf)	Not Listed	5470	N/A
Takeoff Thrust (lbf)	24,000	23,800	- 1%
Cruise TSFC (lbm/hr/lbf)	Not Listed	0.683	N/A
Takeoff TSFC (lbm/hr/lbf)	0.370	0.361	- 2.43%

As shown in Table 1, the baseline model recreation by our team closely matches the values reported in the RFP. However, our team also did work to match the geometry cross section as shown in the RFP. This included various aspects such as matching engine length, engine diameter, and sizing the disks to match. There are also vanes, struts,

and ducting within the engine that our team needed to match. The number of compressor and turbine stages also needed to be matched. The baseline had three booster stages, nine high-pressure compressor stages, one high-pressure turbine stage, and four low-pressure turbine stages. One limitation of GasTurb14 is the fact that in reality, the bypass duct would extend further towards the end of the engine, but GasTurb14 limits the distance to approximately the start of the nozzle. This likely results in a slight underestimate in engine weight. Figure 3 shows our recreated baseline engine cross-section overlayed on top of the cross-section given in the RFP.
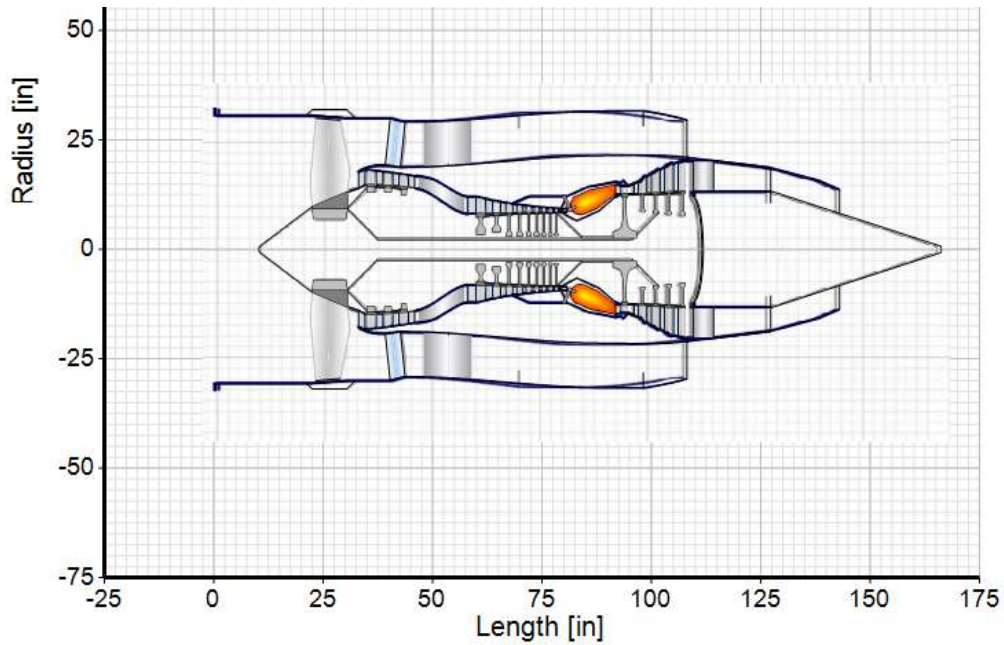
Figure 3: Our team's baseline model creation overlayed on the RFP model [1]

From the recreation of this engine, our team was also able to put together the geometric data, such as size and weight, for the baseline engine. These geometric results are reported in Table 2.

Table 2: Geometric results from the recreation of the CFM56-7B24 engine model in GasTurb14 [1]

	RFP	Recreated Model	Comparison
Dry Weight Less Nozzle (lbm)	5230	5100	-2.49%
Engine Length (in)	98	99	+1.02%
Maximum Engine Diameter (in)	65	64.5	-0.08%

The similarity in results from our team's recreation of the baseline model at takeoff, gave confidence in the cruise values shown in Table 1. The cruise thrust and TSFC in particular were essential for the design of the Dream Stream Propulsion System. The main focus of our team was to reduce the fuel consumption with the new propulsion system, so selecting the design point to be at cruise was the most practical because that is where the aircraft spends the most time over a typical flight profile.

3.2 Dream Stream Propulsion System Design Matrix

A decision matrix was utilized to compare each individual design and determine which had the most potential for best meeting the design objectives and constraints. The design matrix was created in attempt to quantify advantages and disadvantages of the proposed models compared to the baseline model in the five following categories in Table 3 below:

Table 3: Rating criteria for the design matrix

	Weight/Size (size=hard limit, weight=preference)
-2	Significant increase in weight/size over baseline
-1	Some increase in weight/size over baseline
0	No change from baseline
1	Decreased weight/size over baseline
2	Significant decrease in weight/size over baseline
	Fuel Effciency
-2	Expected to significantly increase fuel consumption at cruise
-1	Potentially increased fuel consumption at cruise
0	No change from baseline
1	Potentially decreased fuel consumption at cruise
2	Expected to significantly decrease fuel consumption at cruise
	Technical Feasibility
-2	This technology is not currently being researched
-1	This technology will not be available in 15 years
0	The technology is being researched and is likely available within 15 years
1	The technology is being researched and will be commercially available within 15 years
2	The technology is readily available in the current day (Baseline)
	Complexity
-2	Significant increase in complexity of the engine analysis
-1	Some increase in complexity of the engine analysis
0	No change from baseline
1	Some decrease in complexity of the engine analysis
2	Significant decrease in complexity of the engine analysis
	Power Extraction Flexibility
-2	Model has significant restrictions to extract power compared to the baseline
-1	Potentially reduced power extraction capabilities
0	No change from baseline
1	Potential benefits to extract more power to provide to the aft fan
2	Expect signicantly more capability to extract power and deliver to the aft fan

Weight and size: In terms of size there is a hard limit to the size of the turbofan because it will be mounted below the wing and poses the risk of interference with the ground during takeoff and landing. Increasing the engine weight

increases static loading on the wing and has the potential to negate any possible increases in thrust specific fuel consumption.

Fuel Efficiency: Decreasing fuel consumption was one of key design objectives for the new propulsion system. Ideally a design would have a significant increase in fuel efficiency over the baseline model. A design with little or no increase in fuel efficiency calls into question the necessity for a new design to be produced.

Technical feasibility: Relates to the design of each component to what is currently being researched and utilized today in industry. Ideally, design features are well researched and readily being deployed into industry applications to ensure the design will perform as expected. A design with little or no corroborating research poses a risk in terms of not knowing if the design will meet the design requirements and objectives.

Complexity: The design matrix quantifies the complexity associated in analysis of the design. Because the project is time limited and because only an introductory amount of analysis can be performed it is advantageous that the design is easier to model and make changes to in order to best meet the design requirements.

Power extraction feasibility: The design matrix quantifies the ease with which power can be extracted from the engines to that of the base model. Because there is a need to provide power the rear fan and onboard systems within the aircraft, it is advantageous that the design be able to easily extract power from the engines.

Weights for each category of the design matrix were then determined with fuel efficiency being of the most importance given the primary objective of the minimizing fuel consumption. Similarly, equal importance was also placed on technical feasibility because of the risk of a design being unable to meet the design objectives due to the technology not being mature enough to enter production. Below fuel efficiency and technical feasibility was the weighting for complexity. This was rated with a higher emphasis because the design needs to be able to be analyzed using the tools at disposal. Weight and size were given the second lowest rating. Keeping the weight as low as possible is desired, however adding features to increase fuel efficiency can increase the weight, so keeping this category low encourages the use of next generation technology. The lowest rated category was power extraction

flexibility. This category was ranked the lowest because it was decided that it would be beneficial to be able to easily extract power from the engines to the rear fan, however this was deemed the least impactful parameter for the design of the engine.

Table 4: Turbofan decision matrix

Weighting	0.15	0.275	0.275	0.2	0.1	1
Design	Weight/ Size	Fuel Efficiency	Technical Feasibility	Complexity	Power Extraction Flexibility	Total
Additional booster stage	-1	2	2	0	0	0.95
Additional LP turbine stage	-1	1	2	0	2	0.88
Mixed Nozzle	-2	2	2	-1	0	0.60

3.3 Design Selection

As a result of the design matrix, it was determined that an additional booster design, shown below, be the initial modification to improve engine performance within Gasturb. The additional compression stage allows for a higher pressure and corresponding temperature entering the burner reducing the fuel needed to reach the same outlet temperature leading to a potential decrease in TSFC. The addition of a single stage is also likely not to require a complete redesign of the booster or any adjacent components with the exception of dealing with higher temperatures which is necessary for all of the designs and dealt with material improvements.
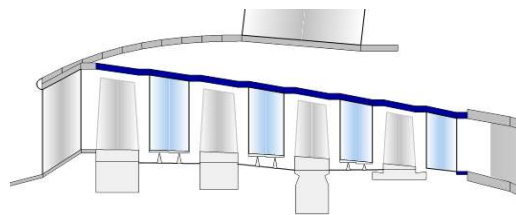
Figure 4: Booster design with additional stage

The purpose of including an additional low pressure turbine spool, as shown below, was to evaluate the effectiveness of dealing with the additional power offtake from the boundary layer ingestion fan given that it is to be

extracted from the low-pressure spool. The design also offers similar tradeoffs to an addition compressor spool but without any notable potential in increased fuel efficiency.
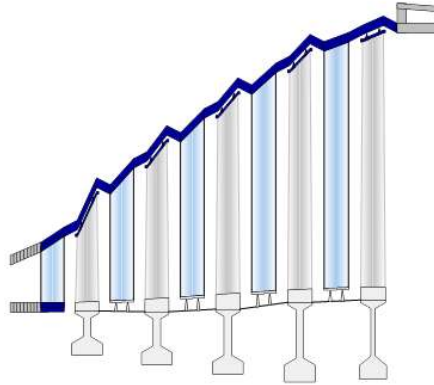
Figure 5: LPT design with additional stage

Changing the nozzle design from unmixed to mixed would be the most radical design evaluated with severe potential for drastically increasing the size and weight of the engine given a likely increase in bypass ratio. A mixed nozzle design, shown below, however would likely provide similar or better results in improving fuel economy given the increased exit velocity of the bypass exit flow.
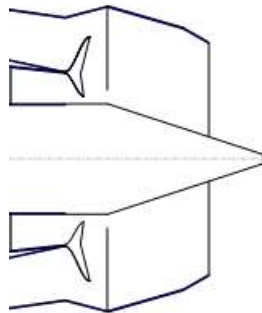
Figure 6: Mixed nozzle turbofan design

3.4 Discussion on Boundary Layer Ingestion

The incorporation of boundary layer ingestion within aircraft propulsion systems is a big point of research in the current day. It provides a very promising future for aircraft propulsion systems, especially in terms of fuel savings. The implementation of boundary layer ingestion on the fuselage is widely researched and debated, however for this design proposal, the fuselage of the NASA STARC-ABL is to be used. This is shown in Figure 7.

Figure 7: Fuselage of the NASA STARC-ABL [1]

The main advantage of incorporating a design as such in Figure 7, is that it is much easier and more efficient to change the velocity of the lower speed boundary layer air [2,3]. Another advantage of boundary layer ingestion is that it essentially increases the bypass ratio of the propulsion system with a reduced drag penalty. The fuselage design shown in Figure 7 incorporates the use of two CFM56-7B24 turbofan engines, with extra power extracted from the turbofan engines to power the aft fan at the rear of the fuselage. NASA has reported that the current design of their aft fan has a pressure ratio of 1.25, a diameter of 1.96 meters, and would require about 2610 kW of power. The NASA STARC-ABL is also designed to ingest about 45% of the momentum deficit from the boundary layer of the fuselage [12]. Research has indicated that there is an optimal range to be within for the percentage of boundary layer ingested in terms of minimizing the average velocity and maximizing the mass flow of the ingested boundary layer air. Typically, industry standard is to assume that the thickness of the boundary layer increases by 1 cm for every 1 m of the fuselage length [13]. The range for optimal momentum deficit captured is estimated to be between 30% and 57%, and the STARC-ABL is towards the average of that range [6]. It has been estimated that the fuel consumption over the span of an average flight can be reduced by upwards of 6% by utilizing boundary layer ingestion. This is all part of NASA's N+3 project which focuses on the future development of subsonic aircraft [5].

This project has long term goals of reducing fuel burn by 50% - 60%, reducing NO_x emissions by up to 80%, and reducing the noise pollution produced by aircraft by 2050 [3].

Due to the promising nature of boundary layer ingestion, many patents for aft fan designs have been granted in aim of trying to best capture the momentum deficit in the boundary layer. One such patent describes the addition of another small core engine at the rear of the fuselage to directly power the aft fan. Though this is not a design that meets the design constraints of the project, the solution aims to mitigate the challenges with implementing boundary layer ingestion. The turbomachinery and power takeoff from the two main engines under the wings is ultimately one of the bigger challenges that needs to be overcome. These challenges include the generator size required to extract large amounts of power from the engine and how the extracted power is routed to the fan motor. Incorporating a third engine at the rear of the aircraft can make it so that no additional power is to be extracted from the base engines, as the third core engine would supply shaft power to the fan directly [14]. As stated, this design is not applicable to the design proposal, but was considered important knowledge because it appears many boundary layer ingestion concepts are opting into this method [14]. Another method that aims to improve the difficulties of boundary layer ingestion is by implementing a two stage, counter-rotating aft fan. The two fan stages would be coupled by a reversed input-outputs gearbox, so that they could be driven in opposite directions. This patent claims that the counter-rotation could eliminate the need for an exit guide vane, which helps keep uniformity in the flow through the fan, and ultimately can possibly help reduce losses by maintaining axial flow through the fan [15].

Other patents have investigated the aft fan blade geometries to utilize as much of the boundary layer flow potential as possible. For example, European patent 3326910A1, describes both passive and active ways to reduce the drag, and provide other benefits to a boundary layer ingesting fan [13]. This patent states that a passive way to best capture the momentum deficit of the boundary layer is to vary the geometry of the fan blades as the radial distance from the center increases. The method prescribed to do this is to vary the incident angle of the fan blades in order to account for the variation in the boundary layer speed as the radial distance from the surface of the fuselage increases. This patent also described an active way of capturing more of the momentum deficit from the boundary layer. This is claimed to be done by individually actuated fan blades, where the incident angle of the blades could

vary as the flight conditions changed and could even be used to provide negative thrust values for landing

conditions. A schematic of this as seen in the patent can be seen in Figure 8.
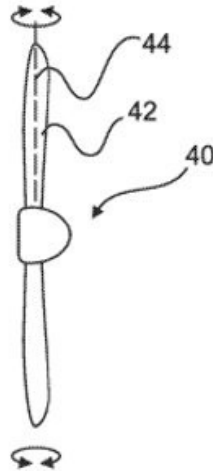
Figure 8: Individually actuated aft fan blades with variable blade geometry as shown in patent EU3326910A1 [13]

Although Figure 8 presents an interesting solution to capturing as much of the boundary layer potential as possible,

it is unlikely necessary, as most of the time in a flight is spent at relatively constant cruise conditions [13].

4. New Propulsion System Design

4.1 System Coupling

To begin our new hybrid-electric model, an electric propulsion system was added directly to the baseline model. To

couple the two systems, the iterations tool was used in GasTurb14 to automatically set the power offtake from the

turbofans to be equal to the power required by the electric fan. As described by the proposal, the power offtake

would be extracted from the low-pressure spool of the turbofan. Since both turbofans are providing power, but only

one turbofan is being analyzed in GasTurb14, the DC Link Electric Power Offtake parameter was used to act as the

power provided from the second turbofan. This was inputted as a negative value so that it was adding power to the

electric fan, not taking it off. An iteration variable was defined so that the power offtake from the low-pressure

spool and the power added by the DC Link parameter were equal, so that each engine provided the exact same

amount of power. Since the thrust provided by the aft fan would be changing in the parametric study, the thrust

provided by the turbofan would also need to change so that the entire system provided the exact thrust determined

from the baseline model. To do so, the iterations tool was used to set the burner exit temperature (T4) to account for the varying thrust requirement in the turbofan. The rotational speeds of the two spools were set using the blade tip speed parameter to ensure that the relative Mach number at the tip of the blades to exceed the baseline model Mach numbers of 1.28 for the high-pressure spool and 1.41 for the low-pressure spool. To prevent the need of a gear box in the generator, an iteration was defined to match the generator speed to the speed of the LP spool. Finally, the hub to tip ratio was iterated so that the aft fan met the design requirement for the inner diameter of 24 inches so that it could fit properly onto the rear of the fuselage. Also, the inlet Mach number for the boundary layer ingestion fan was set to 0.4 [6].

4.2 Aft Fan Trade Studies

Once coupled, we focused on the design of the aft fan before altering the turbofan engines with the goal of minimizing TSFC. This was done by examining the Degree of Hybridization (DoH) parameter to determine what ratio of the total thrust that the electric system should supply. To do so, a parametric study was performed that varied the size of the aft fan by sweeping through a range of values for the fan corrected flow parameter, which is a linear relationship with DoH. The fan pressure ratio was also swept to determine the optimal operating point for the fan. The parametric study was performed and shown in Figure 9 as a plot of effective TSFC as a function of fan corrected flow with contours of constant fan pressure ratios.
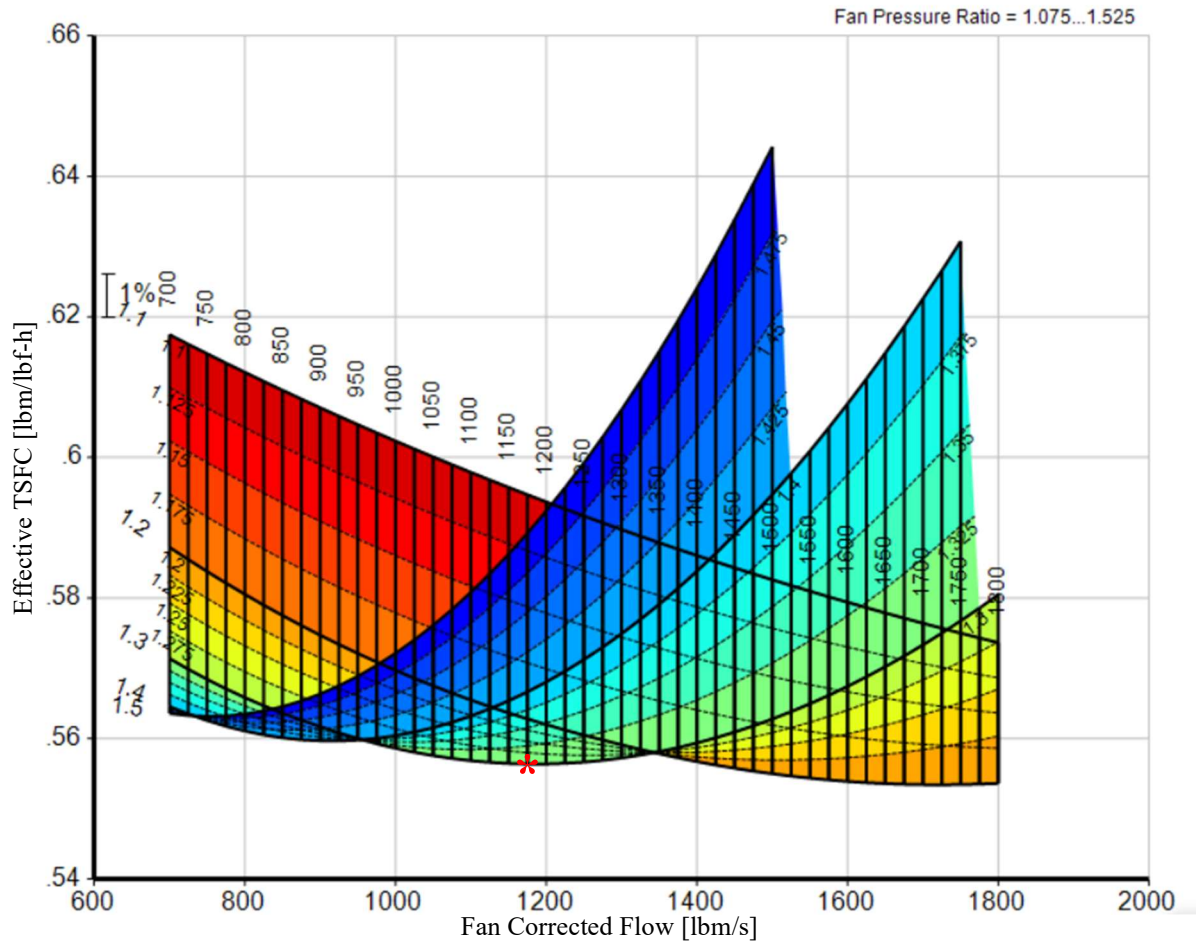
Figure 9: Fan corrected flow and fan pressure ratio parametric study

From the graph, the operating point of the aft fan was selected at a pressure ratio of 1.3 and a fan corrected flow of 1175 [lbm/s], shown by the red star on the graph. While this may not be the lowest TSFC value achievable through changing the aft fan, it corresponds to a smaller aft fan compared to those values further to the right. The values selected correspond to an aft fan with an outer diameter of 86.6 inches and a fan mass of 2028 lb. This fan produces 3258 lbf of thrust, which is 30% of the total thrust required and corresponds to a DoH of 0.38.

4.3 Turbofan Trade Studies

With the fan now designed, changes within the turbofan were examined. First a fourth booster stage was added as determined by the preliminary design matrix. By doing so, this allows us to increase our IP compression ratio from 1.81 to 2.2 while keeping the stage compression at 1.2. A plot of effective TSFC as a function of the booster pressure ratio is shown in Figure 10.
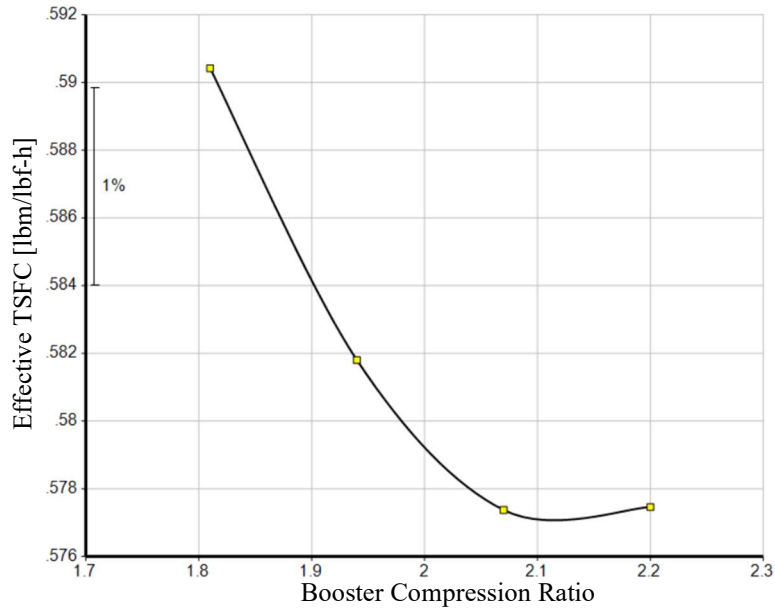
Figure 10: Effective TSFC vs booster compression ratio parametric study

The increase in pressure ratio reduces the effective TSFC from .591 [lbm/lbf-h] to 0.577 [lbm/lbf-h], which is a 2% reduction. Adding a fourth booster stage only has a minimal effect on weight, increasing the weight of the booster from 156 lbm to 195 lbm. While the graph appears to level out, the increase in pressure ratio also increases the overall pressure ratio of the turbofan, which allows the engine core size to be reduced. After performing the following studies, the benefits of adding a fourth booster stage were even greater and this graph became more linear. The two parameters examined next are the bypass ratio and the core engine size, which was changed through the mass flow input parameter of HPC Corrected Flow W25Rstd within GasTurb14. These two parameters were swept through in a parametric study together because they directly affect one another. The results are shown in Figure 11, which is a plot of Effective TSFC as a function of HPC corrected flow with lines of constant bypass ratio. Before the design point could be selected, the same parametric study was analyzed for the output of the maximum engine diameter to ensure that it is equal to or less than the baseline engine maximum diameter. Figure 12 is a plot of the maximum engine diameter as a function of the HPC corrected flow with lines of constant bypass ratio. The selected design point is shown on each graph as the red star.
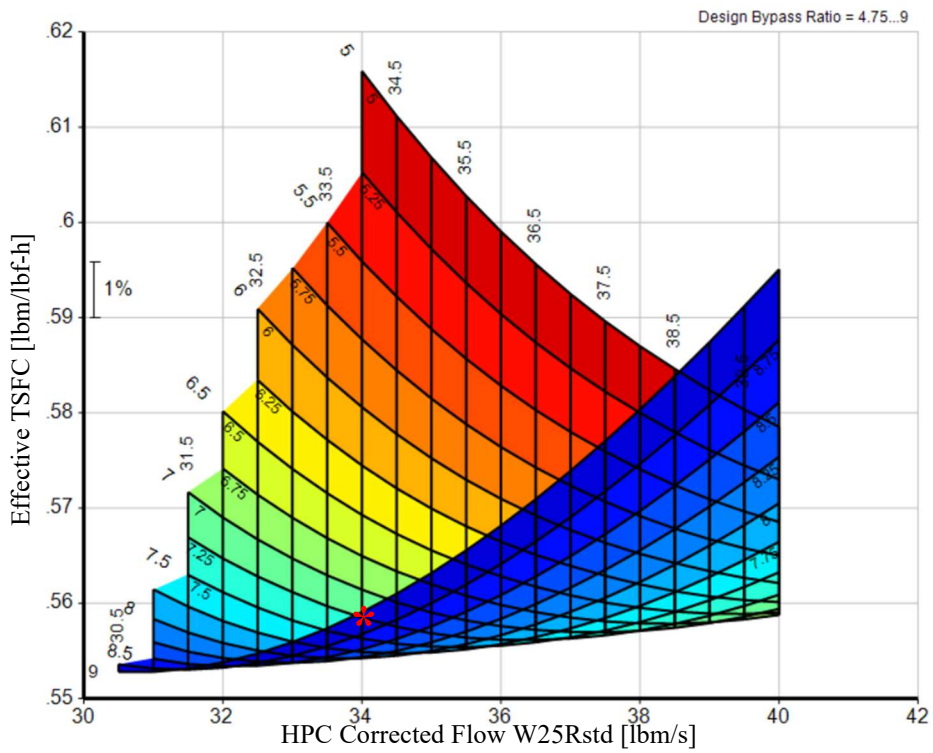
Figure 11: Effective TSFC vs HPC corrected flow and bypass ratio parametric study
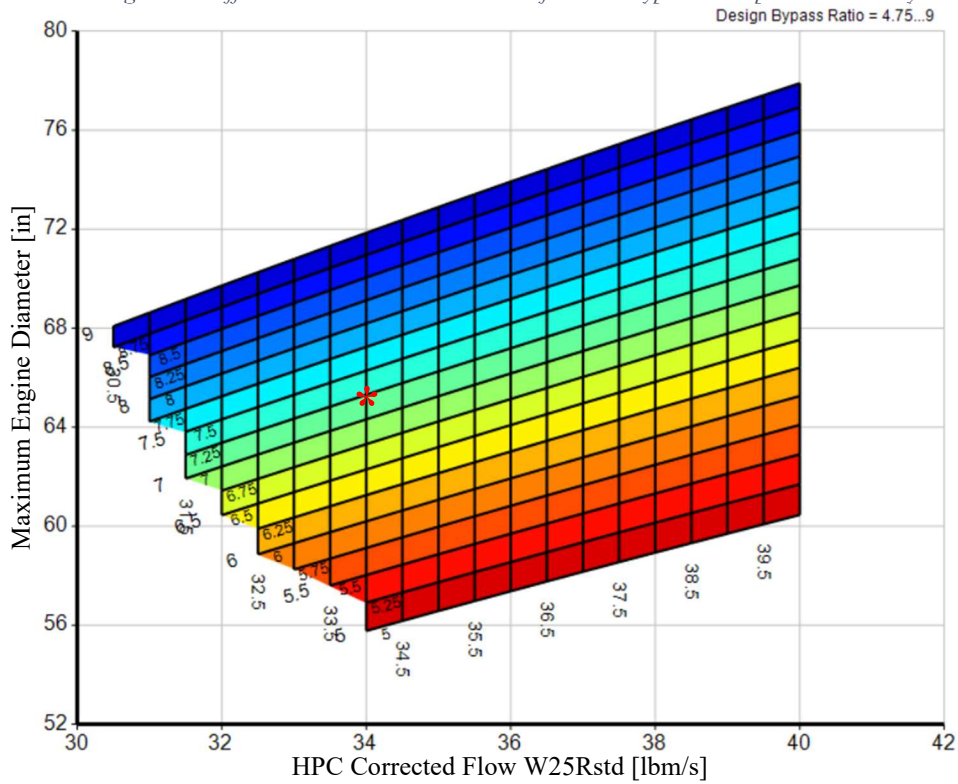
Figure 12: Maximum engine diameter vs HPC corrected flow and bypass ratio parametric study

31

The design point selected is a bypass ratio of 7.25 with an HPC corrected flow of 34 [lbm/s]. This corresponds to an effective TSFC of 0.554 [lbm/lbf-h] and a maximum engine diameter of 65.3 inches. While keeping the engine diameter the same as the baseline, the new proposed engine ensures proper clearance under the wing and also negates implications of increasing the drag force caused by a larger engine. The new model now has a 19% reduction in TSFC. While running the parametric studies, the low-pressure turbine and high-pressure turbine efficiency were set using an isentropic efficiency of 0.9 and 0.8846 respectively. However, as requested by the proposal, velocity diagrams were created by manually calculating the efficiency of each turbine for the final proposed design in Section 5.1. These diagrams can be found in the component design section, with the diagrams being Figure 19Figure 20.

4.2 Materials Selection

The Dream stream design utilizes composites in place of the traditional alloys found within the baseline model. Composite materials have been under development for aerospace applications since the early nineties with research testing, and implementation being performed by NASA, GE, Pratt and Whitney, and numerous other manufactures. Composites can be made to suit almost any environment within a turbofan as seen in the figure below:
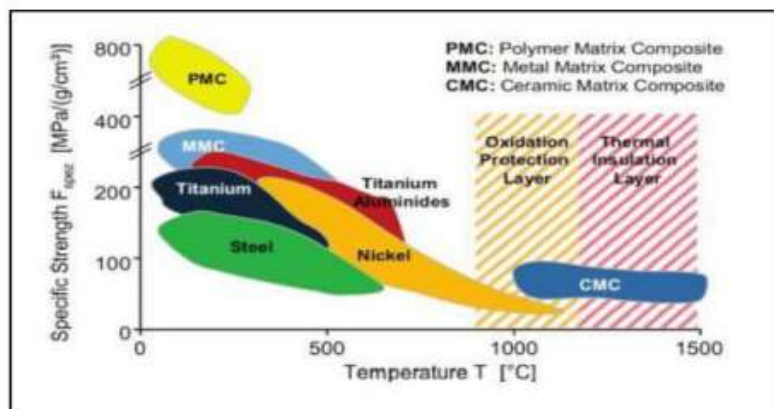
Figure 13: Comparison of composite and traditional turbofan materials [17]

The main concern with the implementation of composite materials within aircraft engines is their ability to handle high stress, high cycle cyclic loading. Early research into composite materials found them susceptible to microcracks during the production process which propagate with thermal shock and cyclic loading leading a decreased lifespan.

Other concerns include oxidation of the fibers at high temperatures and damage done by foreign objects given the generally less impact resistance compared to alloys [16]. More recent studies have proven solutions to the shortcomings to composites using materials, coatings, and the characteristics of the fibers themselves. To make carbon fiber composites stronger, elements like titanium and aluminum are added and coatings utilized to increase toughness. The advancement of minimizing the diameter of the fiber has also allowed for multidirectional patterns, improved chemical resistance, and stronger mechanical interface between the fiber and resin [24].

4.2.1 Inlet/ Bypass Material

The baseline model utilizes a Ti-6Al-4V composite due to its high specific strength for impact resistance and excellent corrosion resistance given the fan and bypass casing are most directly in contact with the elements. Temperature pressure related stresses are of little consideration given operating conditions only slightly exceed the ambient. The Dream Stream Design instead chose to use a fiber reinforced composite (FRC) which has been proven to provide the same strength at roughly half the density as well as being both cheaper and easier to work with. The inspiration for use of FRC's for the bypass and fan casing is the current and next generation GE turbofans which currently utilize laminated fiber fabrics for the bypass [18]. A comparison between the relevant material properties of Ti-6Al-4V and common FRC's are given below:

Table 5: Material Properties of Ti-6Al-4V and common fiber reinforced composite

Material	Ti-6Al-4V [19]	Fiber Reinforced Composite (FRC) [20]
Density (lb/ft^3)	249.7	140.0
Yield Strength, Tensile (ksi)	120	309
Max. Operating temperature (°F)	1112	400

Given FRC's can be designed to be stronger than T-6Al-4V with at minimum half the density and the already proven application in GE's turbofans The Dream Stream design utilizes the material density for FRC's in Table 5 while maintaining the casing thickness which given the increased strength leaves a 100% increase in maximum hoop

stress allowing for any coating and/or matrix refinement to address the problems commonly associated with composites described above such as microcracks due to foreign object damage like bird strikes.

The fan blades and disks were also chosen to be FRC's in place of Ti-6Al-4V for the same reasons as for the casing in addition to further considerations including the continued use of a titanium alloy on the leading edge of the blade to aid in impact resistance to bird strikes. Composites also allow for matrix and composition to vary throughout the blade allowing for better adhesion of protective coating on the surface and allowing increased rigidity through the midsection as shown in Figure 14.
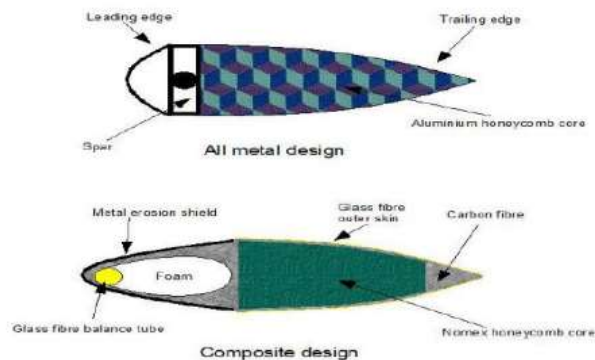
Figure 14: Inlet fan blade cross section comparing metal and composite designs [17]

FRC fan blades have also been practically proven in GE turbofans starting with the GE-90 in 1995 and continuing today with the GE9X. Improvements in the fiber and resins systems throughout the years has been proven to allow for more efficient blade design, and higher strength while decreasing the number of blades needed to produce the same pressure ratio [17]. The Dream Stream design utilizes the same number of blades, however, only changing the material density to match the FRC value in Table 5 which serves as a conservative estimate to what is possible in terms reducing the blade mass with new technologies without knowing the exact construction of the blade.

4.2.2 Booster Material

The Dream Stream design also utilizes FRC's for the booster casing, blades, and disks for all stages. There are no current examples of FRP's being used in low pressure compressors even in the case of the next generation GE turbofans which given the maximum booster output temperature of 370°F current FRCs would be at high risk for creep related failure.

An array of different emerging technologies however will likely make the use of FRPs possible in a very similar manner to the inlet fan. One way this could be made possible is with further advancement in the resin and fiber system making them more stable and less prone to oxidation and microcracks at higher temperatures [16]. Another possibility would be a titanium alloy of metal matrix composite coating which would allow for higher surface temperature resistance while still benefiting in weight reduction.

4.2.3 HPC Material

The dream stream design replaces the INCONCEL 718 casing and compressor blades located in the later stages of the compressor as well as the Ti-6Al-4V blades in the first stages with a titanium aluminide metal matrix composite or similar MMC due to its superior strength to density ratio shown in Figure 15 as well as suitable temperature resistance for the pre burner conditions. MMCs have a comparable density to Ti-6Al-4V while also having double the yield strength meaning components can be designed to be thinner or hollow to aid in heat transfer. In comparison to nickel alloys like INCONEL 718 MMCs are stronger, and a quarter of the density, as shown in Table 6. Given MMCs potential to replace both titanium and nickel-based alloys research in both casing and blades an estimated 15-25% savings in weight has been expected [22] with 15% being used as the conservative estimate.

Nickel based alloys were traditionally required for use in the HP compressor due to the temperature constraints of even the most advanced titanium alloys which peak at around 1112 degrees Fahrenheit which often coincides with the burner inlet temperature. MMCs however can withstand temperatures above 112 degrees Fahrenheit replacing the traditional nickel-based alloys in the later stages of the compressor which allows for the most notable weight reduction [17].

Table 6: Conparison of temperture resistant materials for turbofan design

Material	INCONEL 718 [21]	Titanium Aluminide MMC [22]	Ceramic Matrix Composite (CMC) [16]
Density (lb/ft^3)	499	261	128
Yield Strength, Tensile (ksi)	160	290	79
Max. Operating temperature (°F)	2500	2000+	2900
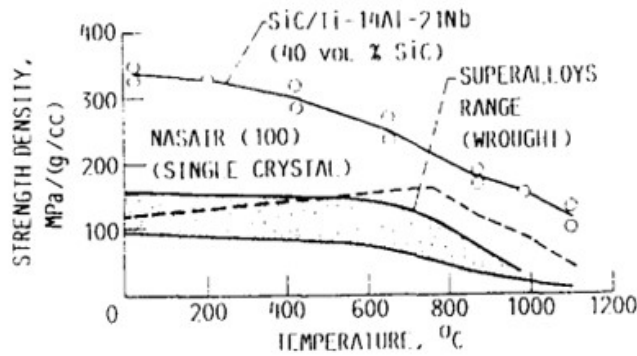
Figure 15: Physical property comparison of MMCs and traditional nickel-based superalloys [22]

4.2.4 Combustor Material

In replacement of INCONEL 718 an emerging ceramic matrix composite (CMC) material was chosen for both the inner and outer casings of the combustor. CMC materials provide two main benefits, first estimated burner outlet temperature increase of 500 degrees Fahrenheit in comparison to traditional nickel-based alloys [24]. CMC materials also offer a significant density reduction in comparison to INCONEL 718 which has been proven though recent research to allow for lighter burners.

To estimate the expected weight savings of the Dream Stream design using CMC casings the burner was modeled as a thin-walled pressure vessel so that the hoop stress could be calculated with the following equation where p represents the component pressure; d, the casing diameter; and t, the casing thickness:

$$\sigma_h = \frac{pd}{2t} \tag{10}$$

Using the casing diameter and thickness of the baseline model an estimated stress and factor of safety regarding the yield strength of INCONEL 718 was determined. Then to maintain the same factor of safety regarding the CMC materials the casing thickness was increased. Using a thin-walled pressure vessel as an assumption means the wall thickness is inversely proportional to the yield strength therefore given current CMC yield strength are about 2 times less then nickel alloys the wall thickness should be expected too roughly double.

36

Another alternative to using only CMC materials for the casing would be to implement MMC casings with CMC liners which is a similar design to currently deployed designs today which use traditional nickel alloys with CMC casings. The first CMC liners were developed in the 1990's with development continuing today with the first planned application being in the GE9X engine [23]. The use of a MMC casing with a CMC lining would likely still allow for the Dream Stream requirements to be met and allow for the increased strength in the casing so that the thickness can be decreased. In either case of using the calculation for CMC materials only or in the case of experimental liners the reported estimation for weight reduction is similar.

4.2.5 Turbine Material

The turbine casing for both the low- and high-pressure spools were chosen to be an emerging CMC material as with the burner as the temperature and pressure requirements are similar in both cases. The use of CMC blades to date have only been experimented with in the low-pressure turbine with the first successful tests being by BE between 2010 and 2015 which utilized a SiC/SiC composite for the blades and citing great potential in decreasing the mass of both blades and disks by lowering the centrifugal forces [23].

The turbine blades could also utilize a hybrid material design much like the inlet fan with an MMC core to accommodate the extra strength requirements required for use in the HP turbine with a CMC shell for temperature and creep resistance. In either case the weight was estimated decrease the same amount as in the booster given MMC materials are more dense serving as an overestimate for a CMC design.

4.2.6 Shaft Material

The dream Stream design uses a Titanium Aluminum Metal Matrix composite (Ti-Al MMC) or equivalent MMC instead of the baselines INCONEL 718 shaft for both the low- and high-pressure spools. Iven MMCs superior strength to density ratio in comparison to INCONEL 718 as described above MMC shafts have the potential of enhanced stiffness, improved rotor dynamics, and a 15-30 percent decrease in weight. Some special design considerations must be considered however which can slightly increase the complexity including the mandatory addition of steel collars for the splines to handle the torsional load and coatings to reduce fatigue during high temperature service [22].

4.2.7 Exhaust/ Nozzle Material

The Dream Stream design replaced INCONCEL 718 with an emerging MMC material the HPC given the design nozzle exit temperature of roughly 1100 degrees Fahrenheit. Like in the case of HPC the increased temperature resistance of titanium aluminide MMCs in comparison to traditional titanium alloys allows it to be used in the nozzle with the benefit of roughly half the density and increased strength.

An alternative to using MMCs is the exhaust and nozzle casing would be with the continued use of CMC materials as with the rest of the components including and following the burner. Many examples of active testing with CMC nozzles already exist with some examples being with the Airbus A320 and Rolls Royce Trent 1000 engines in the 2010s. Current CMC nozzle prototypes offers an estimated weight savings of 15% compared to traditional titanium components in both mixed and unmixed configurations available [23]. However, given the higher strength to density ratio of MMCs in general and their ability to handle temperatures in the 1100 degrees Fahrenheit may tip development towards MMCs.

4.2.8 Weight Analysis

Utilizing the described material changes and estimation for the weight reduction of each component as well as the overall engine is given below:

Table 7: Estimated turbofan mass by component

	Baseline (lbm)	Dream Stream Design (lbm)	Percent Reduction (%)
Fan	821.6	759.4	7.57
Booster	223.4	148.6	33.5
Compressor Innerduct	160.6	81.92	49.0
High Pressure Compressor	416.4	227.7	45.3
Burner	319.8	133.0	58.4
High Pressure Turbine	269.7	169.6	37.1
Turbine innerduct	25.41	10.37	59.2
Low Pressure Turbine	548.6	274.1	50.0
Exhaust	571.0	318.3	44.3

Bypass	507.7	226.4	55.4
Low Pressure Shaft	78.86	52.88	32.9
High Pressure Shaft	18.67	10.08	46.0
Net Turbofan Mass	4474	2854	36.2

Assuming composites advance in as research would indicate decreases of much of 15-50% in mass has been reported in other test cases depending on each component. The high-pressure turbine also acts as the lowest overall reduction by component given it is the area of highest stress in the engine composites applications are just only now starting to be tested in industry.

5. Dream Stream Engine Final Design Analysis

After completing the desired trade studies and implementing material changes, the final hybrid-electric design is defined. The flow path components and their corresponding position within the turbofan are defined in the figures below.

Name	Where it is	Design Mach No	Design Area
St2	Fan Inlet	Calculated by	LPC Design
St22	Booster Inlet	0.5	0
St24	Booster Exit	0.4	0
St25	HP Compressor Inlet	Calculated by	HPC Design
St3	HP Compressor Exit	0.25	0
St4	Burner Exit	0.1	0
St44	HP Turbine Exit	Calculated by	HPT Efficiency
St45	LP Turbine Inlet	0.35	0
St5	LP Turbine Exit	Calculated by	LPT Efficiency
St6	Exit Guide Vane Exit	0.45	0
St8	Core Nozzle Throat	0	0
St13	Bypass Inlet	0.55	0
St16	Bypass Exit	0.5	0
St18	Bypass Nozzle Throat	0	0

Figure 16: Flow path component names and corresponding station numbers
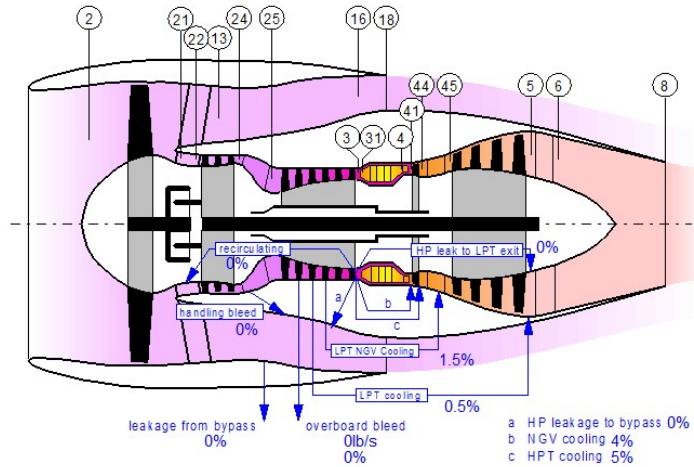
Figure 17: Conceptual cross section highlighting each station number

The following sections display the new hybrid-electrical model's performance at cruise conditions in comparison to the baseline model, the individual component design, and the takeoff performance in comparison to the baseline model.

5.1 Cruise Performance of the Dream Stream Engine (On-Design)

Table 8 below contains the cruise performance of the hybrid-electric Dream Stream Engine in comparison to the baseline engine. The GasTurb14 output window can be found in the appendix.

Table 8: Cruise performance of the new hybrid-electric design compared to the baseline

Parameter	Dream Stream Engine	Baseline Engine	Comparison
Total weight [lbm]	8,376	10,978	-23.7%
Single Turbofan Weight [lbm]	3,139	5,489	-42.8%
Max Diameter [in]	65.3	66.9	---
Max Length [in]	142.9	166	---
Single Turbofan Net Thrust [lbf]	3835	5464	---
Electric Fan Net Thrust [lbf]	3258	---	---
Total Thrust [lbf]	10,928	10,928	---

Thermal Efficiency	0.545	0.522	4.4%
Propulsive Efficiency	0.775	0.727	+6.6%
Effective TSFC [lbm/lbf-h]	0.582	0.683	-14.8%
Fuel Flow Rate [lbm/s]	0.883	1.04	-15.1%
Overall Pressure Ratio	29.9	29.9	---
Degree of Hybridization (DoH)	0.38	---	---
Bypass Ratio	7.25	5.21	---
HPC Corrected Flow [lbm/s]	34	56.5	---
Burner Inlet Temp (T3) (T3 ≤ 1650 R)	1257	1323	---
Burner Exit Temp (T4) (T4 ≤ 3150 R)	3070	2806	---
LP Spool Power Extraction [hp]	3360	---	---

By incorporating boundary layer ingestion, the results show that almost a 15% reduction in Effective TSFC can be achieved. With implementation of new materials, not only does the engine improve in fuel consumption, but its weight is also reduced almost 24%. Figure 18 shows detailed cross-section of the new turbofan engine.
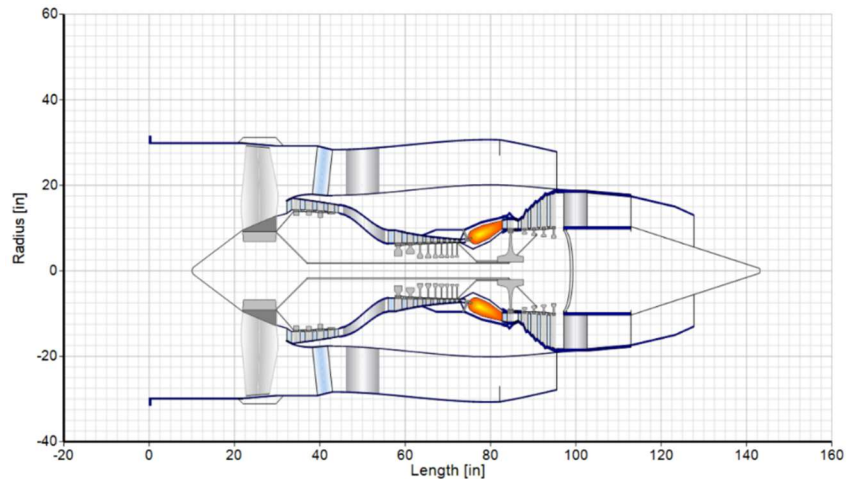
Figure 18: Detailed cross-section of the Dream Stream turbofan

5.2 Individual Component Design

Within this section, the major inputs and outputs for each component are displayed that make up the Dream Stream hybrid-electric engine. The velocity triangle diagrams are included in their respective component design section. The detailed outputs of the turbofan and aft fan, along with the detailed stations output provided by GasTurb14 can be found in Appendix A. Cruise Conditions Detailed GasTurb14 Outputs (On-Design)

5.2.1 Inlet Design

Table 9: Parallel inlet inputs and outputs

Inputs	
Intake Pressure Ratio	0.99
Outputs	
Length [in]	21.97
Cone Length [in]	11.49
Inlet Mass [lbm]	8.29

5.2.2 Fan Design

Table 10: LPC (Fan) inputs and outputs

Inputs	
Inner Fan Pressure Ratio	1.4
Outer Fan Pressure Ratio	1.6
Inner/Outer Fan Isentropic Efficiency	0.9
Fan Tip Speed [ft/s]	1285.88
Fan Inlet Radius Ratio	0.322
Fan Inlet Mach Number	0.58
Outputs	
Fan Tip Relative Mach No	1.41
LP Spool Speed [rpm]	4956

Fan Tip Diameter [in]	59.45
Fan Mass [lbm]	683

5.2.3 Booster Design

Table 11: Booster inputs and outputs

Inputs	
Number of Booster Stages	4
Booster Compression Ratio	2.2
Booster Isentropic Efficiency	0.9208
Outputs	
Booster Mass [lbm]	126
Booster Length [in]	10.8

5.2.4 High-Pressure Compressor Design

Table 12: High-pressure compressor inputs and outputs

Inputs	
Number of Stages	9
HP Compression Ratio	10
HPC Corrected Flow [lbm/s]	34
HPC Tip Speed [ft/s]	1444.26
HPC Isentropic Efficiency	0.9
HPC Inlet Radius Ratio	0.69
HPC Inlet Mach Number	0.45
Outputs	
HPC Tip Relative Mach No	1.28
HPC Spool Speed [rpm]	17716.9

HPC Length [in]	16.9
HPC Total Mass [lbm]	207.4

5.2.5 Burner Design

Table 13: Burner inputs and outputs

Inputs	
Burner Exit Temperature [R]	3070.19
Burner Design Efficiency	0.9995
Burner Pressure Ratio	0.96
Outputs	
Burner Length [in]	9.77
Burner Weight [lbm]	122.4

5.2.6 High-Pressure Turbine Design

Table 14: High-pressure turbine inputs and outputs

Inputs	
Number of Stages	1
HPT Rotor Inlet Diameter [in]	17.6
Last HPT Rotor Exit Diameter [in]	18.8
HPT Exit Radius Ratio	0.77
Outputs	
HPT Total Mass [lbm]	157.66
HPT Disk Stress Margin	72%
HPT Isentropic Efficiency	0.8576
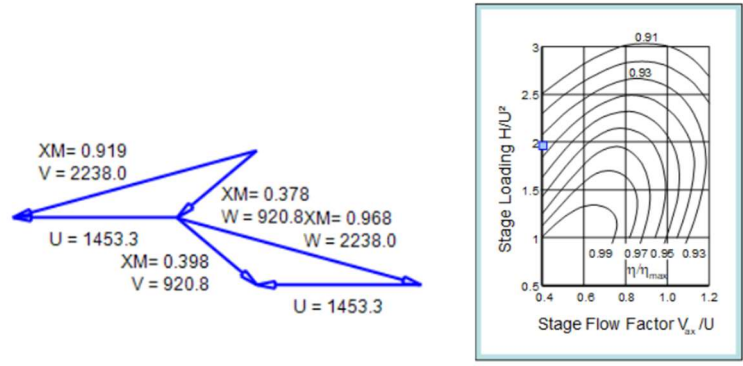
Figure 19: High pressure turbine velocity diagrams and Smith chart

5.2.7 Low Pressure Turbine Design

Table 15:Low-pressure turbine inputs and outputs

Inputs	
Number of Stages	4
HPT Rotor Inlet Diameter [in]	43.95
Last LPT Rotor Exit Diameter [in]	45.1
HPT Exit Radius Ratio	.8
Outputs	
LPT Total Mass [lbm]	235.83
HPT Disk 1 Stress Margin	336%
HPT Disk 2 Stress Margin	281%
HPT Disk 3 Stress Margin	156%
HPT Disk 4 Stress Margin	217%
LPT Isentropic Efficiency	0.8806
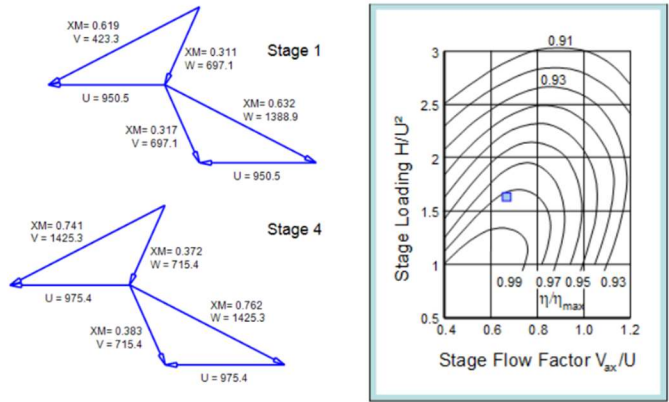
Figure 20: Low pressure turbine velocity diagrams and Smith chart

5.2.8 Bypass Duct Design

Table 16: Bypass duct outputs

Outputs	
Bypass Duct Total Mass [lbm]	203.6
Bypass Nozzle Throat Area [in^2]	1268.97
Bypass Nozzle Throat Mach Number	1.0

5.2.9 Core Nozzle Design

Table 17: Core nozzle outputs

Outputs	
Core Nozzle Total Mass [lbm]	291.9
Core Nozzle Inlet Section Length [in]	10.4
Core Nozzle Convergent Length [in]	4.5
Core Nozzle Throat Area [in^2]	421.57

5.2.10 Boundary Layer Ingestion Fan Design

Table 18: Boundary layer ingestion fan inputs and outputs

Inputs	
Fan Pressure Ratio	1.3
Fan Corrected Flow [lbm/s]	1175
Fan Inlet Mach Number	0.4
Fan Hub to Tip Ratio	0.276989
DC Link El. Power Offtake [hp]	-3360.41
Outputs	
Fan Net Thrust [lbf]	3258.46
Fan Hub Diameter [in]	24
Fan Outer Diameter [in]	86.6

5.3 Takeoff Performance of the Dream Stream Engine (Off-Design)

Once the turbofan model was designed at cruise conditions, it was then taken to takeoff conditions to analyze its performance. Table 19 tabulates the performance parameters of the model at takeoff. The detailed outputs from GasTurb14 including the component station analysis can be found in Appendix B. Takeoff Conditions GasTurb14 Detailed Outputs (Off-Design)

Table 19: Takeoff performance of the hybrid-electric model compared to the baseline model

Parameter	Dream Stream Engine	Baseline Engine	Comparison
Single Turbofan Net Thrust [lbf]	19,446	23,750	---
Electric Fan Net Thrust [lbf]	9,586	---	---
Total Thrust [lbf]	48,478	47,500	+2.1%
Thermal Efficiency	0.475	0.457	+3.9%
Effective TSFC [lbm/lbf-h]	0.300	0.361	-17.0%
Fuel Flow Rate [lbm/s]	2.04	2.38	-14.3%
Overall Pressure Ratio ($OPR_{hybrid} \geq OPR_{baseline}$)	26	26	---
Burner Inlet Temp [R] (T3) ($T3 \leq 1650$ R)	1354.7	1394.29	---
Burner Exit Temp [R] (T4) ($T4 \leq 3150$ R)	3080.2	2800	---
Bypass Ratio	7.43	5.3	---

One adjustment to the model had to be made at takeoff to meet proposal requirements. The overall pressure ratio of the new turbofan was actually less than that of the baseline, so a minimum limiter was set to account for it and the requirement was met. As seen in Table 19, the hybrid electric model actually produces 2% more thrust while still decreasing the TSFC by 17%. To finalize the takeoff performance of our new turbofan, compressor maps were analyzed to ensure that the compressors do not cross the 20% surge margin to ensure safe operation of our turbofan at various off design loading scenarios. The compressor maps can be found below in Figure 21,Figure 22Figure 23.
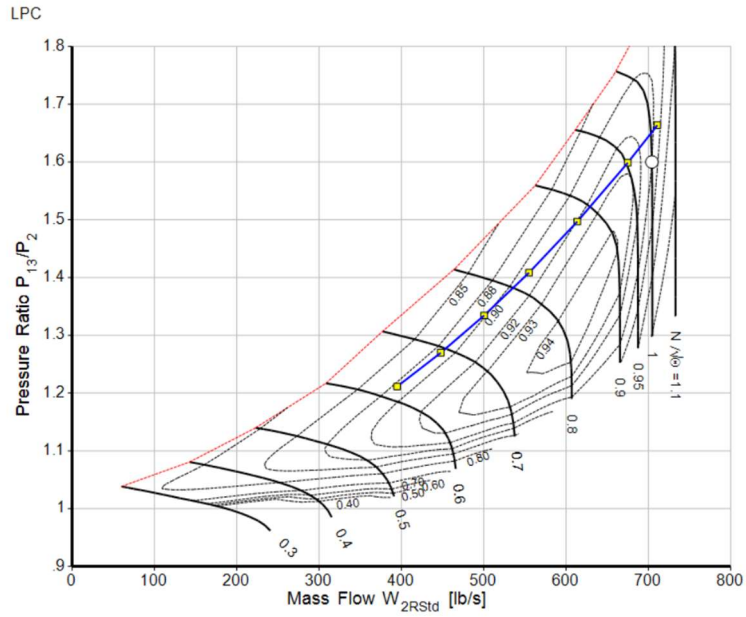
Figure 21: Fan off-design operating line
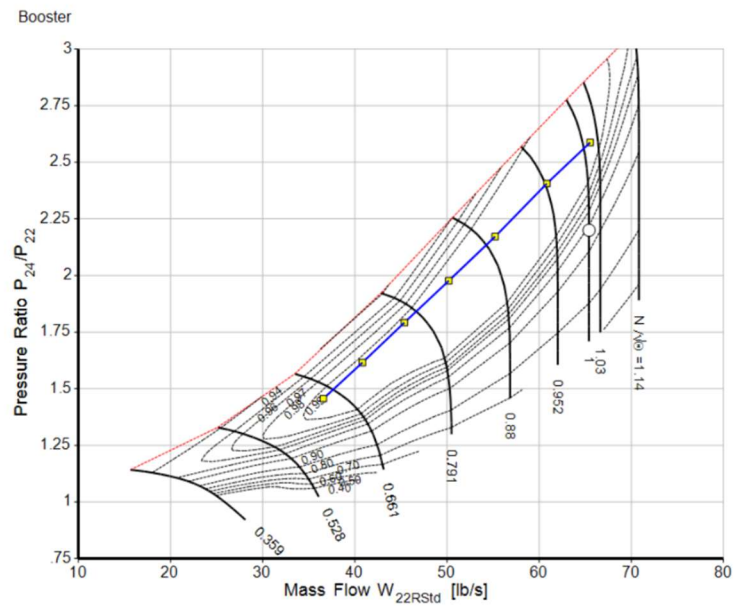
Figure 22: Booster off-design operating line
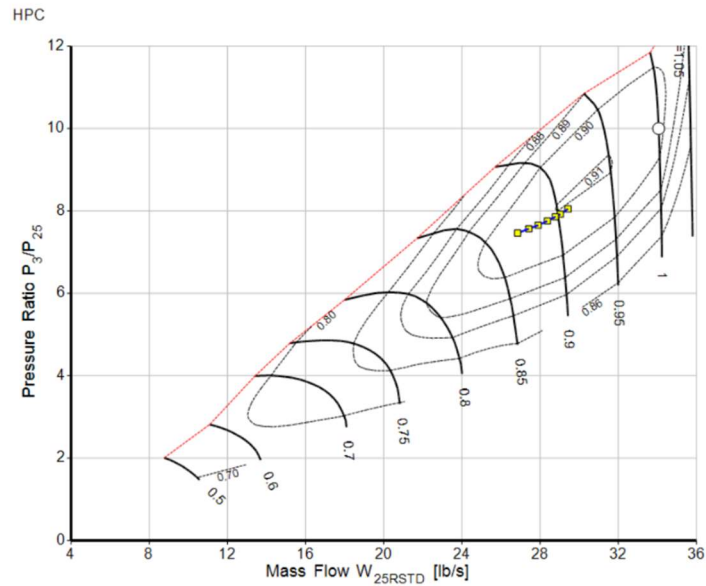
Figure 23: HPC off-design operating line

6. Mission Study

The Boeing 737-800 aircraft is known as an upper medium ranged aircraft, completing long intercontinental flights such as Los Angeles to New York City or Seattle to Miami. These flights can last anywhere from 5 hours to 6 hours long and cover 2400 to 2800 nautical miles [25]. To create our flight profile, it was assumed that the various climb rates during ascent and descent occurred at a constant Mach number and elevation. To account for this, the models were ran off-design at these various conditions to obtain the fuel flow rate for each operating condition. The models were ran at the bottom flight level and at the top flight level for each Mach number so that an average fuel flow rate along the course of each climb could be used to best simulate a flight profile. The final flight profile that was used to compare the two engine designs was a 5 hour and 42-minute flight, with 4 hours and 56 minutes of the flight taking place at cruise conditions. The flight profile can be seen in Figure 24, and the numerical analysis, including the fuel consumption over the course of the flight for each engine is in Figure 25.
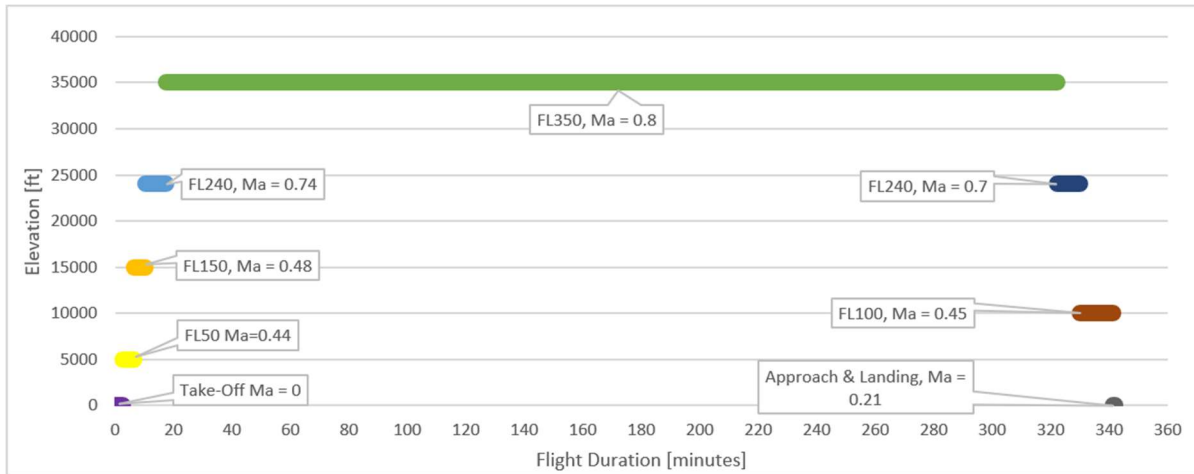
Figure 24: Plot of the approximated mission profile of a Boeing 737-800 aircraft

	Takeoff		Ascent					Cruise		Descent					Landing	Total	
Duration [min]	1	1.7		4.0		3.6		7.3	296	8.8		8.0		11.1	1.0	342	[min]
Altitude [ft]	0	=>	5,000	=>	15,000	=>	24,000	=>	35,000	=>	24,000	=>	10,000	=>	0		
Mach #	0	0.26		0.44		0.48		0.74	0.8	0.7		0.45		0.34	0.21		
ROC [ft/min]		3000		2500		2500		1500		1250		1750		900			
Hybrid Fuel Flow [lb/s]	2.04	2.00		1.66		1.19		1.04	0.87	1.09		1.52		2.13	2.24	19698	[lb fuel]
Baseline Fuel Flow [lb/s]	2.49	2.37		2.03		1.52		1.26	1.06	1.23		1.65		2.22	2.48	23701	[lb fuel]
Fuel Savings	18%	15%		18%		22%		17%	18%	11%		8%		4%	10%	17%	

Figure 25: Mission performance comparison of total fuel burn between the new hybrid model and the baseline model

The mission study supports the design results and further exhibits the benefits of adding a boundary layer ingestion fan. The hybrid-electric model consumes 17% less fuel than the baseline engine over the entire course of flight.

7. Conclusion

Although the implementation of boundary layer ingestion in aircraft shows promising benefits to the fuel consumption of aircraft engines, there is still much research that needs to be done on incorporating this into the fuselage and how it effects the wake of the aircraft. The Dream Stream Propulsion system design showed to be a viable solution to the design proposal, as it proved to be a safe design that met all thrust targets at every point across its flight profile.

The design of the Dream Stream Propulsion system aimed to minimize the specific fuel consumption at cruise by changing main variables such as bypass ratio, maximum operating temperature (T4) and overall pressure ratio. Using GasTurb14 to run trade studies, and verifying the thermodynamic results with MATLAB functions, our team

was able to reduce fuel consumption of the engine significantly. By implementing new materials, our team was also able to increase the thermal efficiency as a result of increasing T4.

Our team's important objective of keeping the frontal area of the engine the same was also achieved. This was a result of increasing the thermal efficiency and making the core of the engine smaller. This allowed us to increase the bypass ratio while maintaining the same engine diameter. This was done in consideration of ground clearance on takeoff, as well as minimizing drag increases of the new propulsion system.

The following table provides the improvements that can be gained by using the Dream Stream Propulsion System.

Table 20: Characteristics of the Dream Stream Propulsion System compared to the baseline engine

Parameter	Baseline (CFM56-7B24)	Dream Stream Propulsion System	Comparison
Cruise TSFC [lbm/lbf-h]	0.683	0.582	- 14.2%
Total Fuel Consumed During Flight [lbm]	23,701	19,698	- 17%
Engine Weight [lbm]	5,489	3,139	- 42.8%
Propulsion System Weight [lbm]	10,978	8,376	- 23.7%
Thermal Efficiency	0.522	0.545	+ 4.4%
Propulsive Efficiency	0.727	0.775	+ 6.6%

This design also meets all the stress margin specifications and surge margin specifications at all points throughout its flight.

References

[1] American Institute of Aeronautics and Astronautics, "Design Competitions," *American Institute of Aeronautics and Astronautics*, 2022. [Online]. Available: https://www.aiaa.org/get-involved/students-educators/Design-Competitions

[2] Samuelsson, S., and Grönstedt, T.. "Performance Analysis of Turbo-Electric Propulsion System with Fuselage Boundary Layer Ingestion". Aerospace Science and Technology. 109, 106412, Aerospace Science and Technology, 2021. Available: Science Direct, https://doi.org/10.1016/j.ast.2020.106412 [Accessed: Oct. 6, 2022].

[3] Menegozzo, L., and Benini, E.. "Boundary Layer Ingestion Propulsion: A Review on Numerical Modeling". The American Society of Mechanical Engineers. Journal of Engineering for Gas Turbines and Power 142, no. 12 (2020). Available: ASME, https://ezproxy.msoe.edu:2321/gasturbinespower/article/142/12/120801/1086307/Boundary-Layer-Ingestion-Propulsion-A-Review-on [Accessed: Oct. 6, 2022]

[4] Onal, O., Turan, O.. "Calculation and Comparison of a Turbofan Engine Performance Parameters with Various Definitions". World Academy of Science, Engineering and Technology, Open Science Index 118, International Journal of Aerospace and Mechanical Engineering, 2016. Available: WASET, https://publications.waset.org/10005503/calculation-and-comparison-of-a-turbofan-engine-performance-parameters-with-various-definitions [Accessed: Sept. 26, 2022].

[5] NASA, "Turbofan Engine," *NASA*, 2021. [Online]. Available: https://www.grc.nasa.gov/www/k-12/airplane/aturbf.html [Accessed Sept. 26, 2022].

[6] P. Hill and C. Peterson, *Mechanics and Thermodynamics of Propulsion*, 2nd ed. Hoboken, NJ: Pearson, 1992.

[7] Sforza, P.M.. *Theory of Aerospace Propulsion*, 2nd ed.. Elsevier, 2017. [E-book] Available: Science Direct, https://doi.org/10.1016/B978-0-12-809326-9.00009-9 [Accessed: Sept. 26, 2022]

[8] Kandebo, S.W., "Similar But Different.". EbscoHost, Aviation Week & Space Technology, 160, no. 20 (2004). Available: EbscoHost, https://web.s.ebscohost.com/ehost/detail/detail?vid=4&sid=1065c397-6262-4c52-bfac-ceb02779bed1%40redis&bdata=JkF1dGhUeXBlPWNvb2tpZSxpcCxjcGlkJmN1c3RpZD1zNjIyMjE2NiZzaXRlPWVob3N0LWxpdmUmc2NvcGU9c2l0ZQ%3d%3d#AN=500991397&db=aps [Accessed: Nov. 7, 2022].

[9] Dik, A., Bitèn, N., Zaccaria, V., Aslanidou, I., Kyprianidis, K.G.. "Conceptual Design of a 3-Shaft Turbofan Engine with Reduced Fuel Consumption for 2025". Elsevier, Energy Procedia, 142 (2017). Available: Science Direct, https://www.sciencedirect.com/science/article/pii/S1876610217363129 [Accessed, Oct. 17, 2022].

[10] Doyle, Andrew. "R-R Details Three-Shaft RB285 Study for 150-Seat Market." Flight Global, 27 Dec. 2019. [Online]. Available: https://www.flightglobal.com/r-r-details-three-shaft-rb285-study-for-150-seat-market/82876.article. [Accessed: Oct. 28, 2022].

[11] Barbosa, C.B., "Ultra high bypass ratio engine technology review – the efficiency frontier for the turbofan propulsion". In Proc. SAE BRASIL 2021 Web Forum, 2021.

[12] Welstead, Jason, Jim Felder, Mark Guynn, Bill Haller, Mike Tong, Scott Jones, Irian Ordaz, Jesse Quinlan, and Brian Mason. Overview of the NASA STARC-ABL (Rev. B) Advanced Concept. Hampton: NASA/Langley Research Center, 2017. Available: https://ezproxy.msoe.edu/login?url=https://ezproxy.msoe.edu:2256/other-sources/overviewnasa-starc-abl-rev-b-advanced-concept/docview/2128052545/se-2. [Accessed, Sept. 26, 2022].

[13] Trahmer Bernd. Aircraft having a drag compensation device based on a boundary layer ingesting fan. EU Patent EP3326910A1, filed November 29, 2016 and issued May 30, 2018.

[14] Hoisington, Zachary. System and method for operating a boundary layer ingestion fan. US Patent 11111029B2, filed July 28, 2018 and issued September 7, 2021.

[15] Chandler, Jesse and Suciu Gabriel. Aft counter-rotating boundary layer ingestion engine. EU Patent 3557036B1, filed March 26, 2019 and issued February 24, 2021.

[16] Petko, J,. and Kiser, D.. "Characterization of C/SiC Ceramic Matrix Composites (CMCs) with Novel Interface Fiber Coatings" *National Aeronautics and Space Administration*, 2002. [Online]. Available: https://ntrs.nasa.gov/api/citations/20020072848/downloads/20020072848.pdf

[17] K. Suhrutha and G. Srinivas, "Recent Developments of Materials used in Air breathing and Advanced Air breathing Engines" IOP Conference Series: Materials Science and Engineering, 01-Jun-2020. [Online]. Available: https://iopscience.iop.org/article/10.1088/1757-899X/872/1/012082

[18] Okura, Takehiro. "Materials for Aircraft Engines" University of Colorado Boulder, 2015. [Online]. Available: https://www.colorado.edu/faculty/kantha/sites/default/files/attached-files/73549-116619_-_takehiro_okura_-_dec_17_2015_1027_am_-_asen_5063_2015_final_report_okura.pdf

[19] "Titanium Ti-6Al-4V (Grade 5), Annealed". MatWeb. [Online]. Available: https://www.matweb.com/search/DataSheet.aspx?MatGUID=10d463eb3d3d4ff48fc57e0ad1037434&ckck=1

[20] "Overview of materials for Epoxy/Carbon Fiber Composite". MatWeb. [Online]. Available: https://www.matweb.com/search/datasheet.aspx?matguid=39e40851fc164b6c9bda29d798bf3726

[21] "Special Metals INCONEL Alloy 718". Aerospace Specification Metals Incorporated. [Online]. Available:

https://asm.matweb.com/search/SpecificMaterial.asp?bassnum=NINC34

[22] Singerman, S. A., J. J. Jackson, and M. Lynn. "Titanium metal matrix composites for aerospace applications."

Superalloys 1996, proceedings of eighth international symposium on superalloys. 1996. Available:

https://www.tms.org/superalloys/10.7449/1996/superalloys_1996_579_586.pdf

[23] Wehrel, Patrick. "Technological Level of CMC Components for Stationary Gas Turbines and Aero-Engines"

German Aerospace Center, institute of Propulsion Technology. 2022. Available:

https://elib.dlr.de/186166/1/Wehrel_Technological%20Level%20of%20CMC%20Components%20for%20

Stationary%20Gas%20Turbines%20and%20Aero-Engines.pdf

[24] Levine, S.R.. "Ceramic Composites- Enabling Aerospace Materials". NASA Technical Memorandum 105599.

1992. Available: https://ntrs.nasa.gov/api/citations/19920018135/downloads/19920018135.pdf

[25] "B738". Aircraft Performance Database. Available:

https://contentzone.eurocontrol.int/aircraftperformance/details.aspx?ICAO=B738&NameFilter=737

Appendix

A. Cruise Conditions Detailed GasTurb14 Outputs (On-Design)

```
             W        T        P      WRstd
Station    lb/s       R      psia     lb/s      FN       =   3834.68 lb
 amb               393.85    3.458              TSFC     =    0.8290 lb/(lb*h)
   2     270.216   444.38    5.220   704.158    WF       =    0.88302 lb/s
  13     237.462   515.44    8.352   416.533    s NOX    =    0.3888
  21      32.753   494.27    7.308    64.298
  22      32.753   494.27    7.235    64.947    Core Eff =    0.5453
  24      32.753   629.65   15.917    33.320    Prop Eff =    0.7748
  25      32.753   629.65   15.598    34.000    BPR      =    7.2500
   3      32.098  1257.30  155.984     4.708    P2/P1    =    0.9900
  31      29.151  1257.30  155.984              P3/P2    =     29.88
   4      30.034  3070.18  149.745     7.171    P5/P2    =    1.2311
  41      31.344  3001.94  149.745     7.400    P16/P13  =    0.9800
  43      31.344  2456.99   52.007              P16/P6   =    1.32671
  44      32.981  2402.71   52.007              P16/P2   =    1.56800
  45      33.473  2384.35   51.485    20.486    P6/P5    =    0.96000
  49      33.473  1563.54    6.426              A8       =    421.57 in²
   5      33.636  1561.30    6.426   133.455    A18      =   1268.97 in²
   8      33.636  1561.30    6.169   139.015    XM8      =    0.96374
  18     237.462   515.44    8.185   425.034    XM18     =    1.00000
Bleed      0.000  1257.30  155.984              wBld/W2  =    0.00000
--------------------------------------------    CD8      =    0.97767
Efficiency         isentr  polytr   RNI   P/P   CD18     =    0.97600
  Outer LPC        0.9000  0.9064  0.426 1.600   PWX      =     150.0 hp
  Inner LPC        0.9000  0.9047  0.426 1.400   V18/V8,id=    0.68387
  IP Compressor    0.9208  0.9291  0.521 2.200   WBLD/W22 =    0.00000
  HP Compressor    0.9000  0.9257  0.843 10.000  Wreci/W25=    0.00000
  Burner           0.9995                 0.960  Loading  =    100.00 %
  HP Turbine       0.8576  0.8421  1.310 2.879   WCHN/W25 =    0.04000
  LP Turbine       0.8806  0.8504  0.587 8.011   WCHR/W25 =    0.05000
-----------------------------------------------  WCLN/W25 =    0.01500
HP Spool mech Eff 0.9900  Nom Spd  17717 rpm     WCLR/W25 =    0.00500
LP Spool mech Eff 0.9900  Nom Spd   4957 rpm     WBLD/W25 =    0.00000
-----------------------------------------------  WLkBy/W25=    0.00000
P22/P21=0.9900 P25/P24=0.9800 P45/P44=0.9900     WlkLP/W25=    0.00000
-----------------------------------------------
hum [%]    war0      FHV     Fuel
  0.0    0.00000   18552.4   Generic
At the gas turbine design point, 3360.41 hp from the LP Spool
are provided to the electric propulsion system.
```

Figure 26: GasTurb14 detailed turbofan outputs at cruise

```
Fan Net Thrust        = 9586.54 lb      Fan Pressure Ratio    =   1.14
Fan Gross Thrust      = 9586.54 lb      Fan Corr. Flow        = 658.07 lb/s
Fan Isentr. Efficiency =  0.79          Fan Corr. rel. Speed  =   0.69
Fan Prop. Efficiency  =   0.00

-----------------------------------------------------------------------

                       Power Output   Losses      Efficiency
                            hp          hp

Overall System           3360.41     1139.55        0.814
-------------------
Fan Gear Box             5581.28        0.00         1.000
Electric Motor           5581.28      877.51         0.864

El. System               6458.78      130.65         0.980
 - Inverter              6458.78       98.36         0.985
 - Rectifier             3196.73       32.29         0.990

Generator                3229.02      131.40         0.961
Generator Gear Box       3360.41        0.00         1.000

At the DC Bus an electric Power of 3360.4 hp is fed into the electric system.

-----------------------------------------------------------------------

The gas turbine provides 3360.4 hp of shaft power to the
electric propulsion system.
```

Figure 27: GasTurb14 detailed electric fan outputs at cruise

	Units	St 2	St 22	St 24	St 25	St 3	St 4	St 44	St 45	St 5	St 6	St 8	St 13	St 16	St 18
Mass Flow	lb/s	270.216	32.7534	32.7534	32.7534	32.0984	30.0336	32.9814	33.4727	33.6364	33.6364	33.6364	237.462	237.462	237.462
Total Temperature	R	444.378	494.273	629.653	629.653	1257.3	3070.18	2402.71	2384.35	1561.3	1561.3	1561.3	515.445	515.445	515.445
Static Temperature	R	416.31	470.697	610.227	605.264	1242.98	3065.84	2379.31	2341.55	1529.86	1510.58	1350	485.993	490.861	429.396
Total Pressure	psia	5.21998	7.23489	15.9168	15.5984	155.984	149.745	52.0068	51.4846	6.42642	6.16936	6.16936	8.35197	8.18493	8.18493
Static Pressure	psia	4.15558	6.09881	14.258	13.5778	149.507	148.787	49.8329	47.5749	5.92156	5.40205	3.45834	6.79955	6.89979	4.32276
Velocity	ft/s	580.321	531.864	484.058	542.376	426.703	260.008	591.984	800.365	658.773	836.692	1699.63	594.455	543.106	1016.1
Area	in²	2488.73	253.573	154.505	143.622	33.3663	126.983	141.917	109.817	703.775	599.754	412.159	1523.27	1659.52	1238.52
Mach Number		0.580008	0.5	0.4	0.450004	0.25	0.1	0.256929	0.35	0.352204	0.45	0.963656	0.55	0.5	1
Density	lb/ft³	0.026942	0.034972	0.063064	0.060548	0.324646	0.130989	0.056531	0.05484	0.010447	9.6524E-3	6.9144E-3	0.037763	0.037939	0.027172
Spec Heat @ T	BTU/(lb*R)	0.239848	0.240007	0.241189	0.241189	0.256822	0.310889	0.298807	0.298253	0.27683	0.27683	0.27683	0.240075	0.240075	0.240075
Spec Heat @ Ts	BTU/(lb*R)	0.239759	0.239932	0.240964	0.240907	0.256367	0.310836	0.298364	0.297445	0.275784	0.275144	0.269605	0.239981	0.239996	0.2398
Enthalpy @ T	BTU/lb	-22.1298	-10.1659	22.4081	22.4081	177.887	715.491	509.398	503.619	266.147	266.147	266.147	-5.08937	-5.08937	-5.08937
Enthalpy @ Ts	BTU/lb	-28.8598	-15.8189	17.7256	16.5294	174.249	714.14	502.395	490.818	257.474	252.157	208.419	-12.1512	-10.9839	-25.7221
Entropy Function @ T		-0.659571	-0.287637	0.561029	0.561029	3.04834	6.92359	5.81091	5.77441	3.99845	3.99845	3.99845	-0.141042	-0.141042	-0.141042
Entropy Function @ Ts		-0.887613	-0.458458	0.450975	0.422297	3.00593	6.91717	5.76821	5.69544	3.91663	3.86563	3.41964	-0.346683	-0.311845	-0.779442
Exergy	BTU/lb	11.8428	22.5769	53.524	52.9781	203.466	635.277	430.671	425.605	179.895	178.792	178.792	27.572	27.0261	27.0261
Gas Constant	BTU/(lb*R)	0.068607	0.068607	0.068607	0.068607	0.068607	0.068606	0.068606	0.068606	0.068606	0.068606	0.068606	0.068607	0.068607	0.068607
Fuel-Air-Ratio		0	0	0	0	0	0.030292	0.02751	0.027095	0.02696	0.02696	0.02696	0	0	0
Water-Air-Ratio		0	0	0	0	0	0	0	0	0	0	0	0	0	0
Inner Radius	in	9.5728	14.2833	13.5691	6.44555	6.54259	9.87302	9.87302	9.87302	10.3667	10.3667	10.3667	17.6793	20.12	19.1219
Outer Radius	in	29.7292	16.8738	15.2726	9.34138	7.31379	11.7429	11.9436	11.5079	18.2068	17.2736	12.8453	28.2387	30.546	27.7412
Axial Position	in	21.9687	21.9687	44.6588	56.0568	74.0562	82.7781	85.528	86.4956	95.5846	112.881	127.703	42.9394	82.1209	95.532

Figure 28: GasTurb14 detailed turbofan station outputs at cruise

B. Takeoff Conditions GasTurb14 Detailed Outputs (Off-Design)

```
            W         T         P       WRstd
Station   lb/s        R        psia      lb/s       FN        =   19723.14 lb
amb                 518.67    14.696               TSFC      =       0.3729 lb/(lb*h)
    2    667.554    518.67    14.549    674.297    WF        =      2.04303 lb/s
   13    588.341    598.52    23.245    399.577    s NOX     =       0.7321
   21     79.213    574.76    20.346     60.230    P5/P2     =       1.3148 EPR
   22     79.213    574.76    20.168     60.763    Core Eff  =       0.4753
   24     79.212    735.50    48.470     28.600    Prop Eff  =       0.0000
   25     79.212    735.50    47.755     29.028    BPR       =       7.4274
    3     77.628   1354.70   378.272      4.874    P2/P1     =       0.9900
   31     70.499   1354.70   378.272               P3/P2     =      26.00
    4     72.542   3080.18   362.058      7.175    P5/P2     =       1.3148
   41     75.711   3014.80   362.058      7.409    P16/P13   =       0.9816
   43     75.711   2475.99   127.493               P16/P6    =       1.22670
   44     79.671   2424.84   127.493               P16/P2    =       1.56827
   45     80.859   2407.36   126.239     20.280    P6/P5     =       0.97236
   49     80.859   1640.26    19.129               A8        =       421.57 in²
    5     81.255   1638.14    19.129    110.940    A18       =      1268.97 in²
    8     81.255   1638.14    18.600    114.094    XM8       =       0.60351
   18    588.341    598.52    22.817    407.069    XM18      =       0.81843
Bleed     0.000   1354.70   378.272               WBld/W2   =       0.00000
--------------------------------------------      CD8       =       0.95304
Efficiency    isentr   polytr    RNI      P/P      CD18      =       0.96399
Outer LPC     0.9284   0.9330   0.990    1.598     PWX       =       150.0 hp
Inner LPC     0.9284   0.9338   0.990    1.398     V18/V8,id =       0.81267
IP Compressor 1.0129   1.0114   1.215    2.403     WBLD/W22= =       0.00000
HP Compressor 0.9099   0.9310   2.143    7.921     Wreci/W25=       0.00000
Burner        0.9999                     0.957     Loading   =      40.99 %
HP Turbine    0.8533   0.8376   3.152    2.840     WCHN/W25  =       0.04000
LP Turbine    0.8823   0.8558   1.425    6.599     WCHR/W25  =       0.05000
--------------------------------------------      WCLN/W25  =       0.01500
HP Spool mech Eff 0.9900  Speed     17269 rpm      WCLR/W25  =       0.00500
LP Spool mech Eff 0.9900  Speed      5092 rpm      WBLD/W25  =       0.00000
--------------------------------------------      WLkBy/W25=       0.00000
P22/P21=0.9912 P25/P24=0.9853 P45/P44=0.9902      WlkLP/W25=       0.00000
--------------------------------------------
hum [%]    war0      FHV     Fuel
   0.0    0.00000   18552.4   Generic

Electric propulsion system (3360.41 hp) connected to LP Spool.
```

Figure 29: GasTurb14 detailed turbofan outputs at takeoff

```
Fan Net Thrust          = 3258.46 lb     Fan Pressure Ratio   = 1.30
Fan Gross Thrust        = 14169.92 lb      Fan Corr. Flow      = 1175.00 lb/s
Fan Isentr. Efficiency  = 0.85
Fan Prop. Efficiency    = 0.87

-------------------------------------------------------------------------

                          Power Output    Losses      Efficiency     Mass
                              hp            hp                         lb

Overall System             6229.88        490.94         0.908       2098.0
-------------------
Fan Gear Box               6229.88          0.00         1.000          0.0
Electric Motor             6229.88        225.95         0.965        614.5

El. System                 6455.84        130.57         0.980       1096.8
 - Inverter                6455.84         98.31         0.985        169.8
 - Cable to Fan            6554.15          0.00         1.000        538.7
 - SSPC to Fan             6554.15          0.00         1.000         28.0
 - SSPC to Generator       3193.74          0.00         1.000         13.7
 - Cable to Generator      3193.74          0.00         1.000        262.5
 - Rectifier               3193.74         32.26         0.990         84.0

Generator                  3226.00        134.42         0.960        386.7
Generator Gear Box         3360.41          0.00         1.000          0.0

At the DC Bus an electric Power of 3360.4 hp is fed into the electric system.

-------------------------------------------------------------------------

At the electric propulsion system design point, 3360.4 hp
of shaft power are required from the gas turbine.
```

Figure 30: GasTurb14 detailed aft fan outputs at takeoff

	Units	St 2	St 22	St 24	St 25	St 3	St 4	St 44	St 45	St 5	St 6	St 8	St 13	St 16	St 18
Mass Flow	lb/s	667.554	79.2127	79.2124	79.2125	77.6282	72.5421	79.6712	80.8594	81.2555	81.2555	81.2555	588.341	588.341	588.341
Total Temperature	R	518.67	574.758	735.502	735.502	1354.7	3080.18	2424.84	2407.36	1638.14	1638.14	1638.14	598.522	598.522	598.524
Static Temperature	R	489.802	551.804	719.738	716.194	1338.44	3075.82	2401.68	2365.05	1616.61	1605.22	1545.12	568.22	573.151	527.997
Total Pressure	psia	14.549	20.1675	48.4697	47.7555	378.272	362.058	127.493	126.239	19.1289	18.6002	18.6002	23.2446	22.8168	22.8168
Static Pressure	psia	11.9098	17.478	44.8759	43.4548	361.371	359.74	122.276	116.864	18.123	17.1289	14.6959	19.3679	19.5971	14.696
Velocity	ft/s	588.537	526.181	438.696	484.971	459.734	260.593	588.277	794.99	549.461	677.374	1134.41	604.557	553.188	921.905
Area	in²	2488.73	253.573	154.505	143.622	33.3663	126.983	141.917	109.817	703.775	599.754	401.783	1523.27	1659.52	1223.28
Mach Number		0.542408	0.456998	0.33414	0.370288	0.260116	0.100034	0.254105	0.345893	0.286186	0.353978	0.603514	0.517508	0.471516	0.818426
Density	lb/ft³	0.065629	0.085491	0.168287	0.163765	0.728732	0.315681	0.137419	0.133371	0.030258	0.028801	0.025672	0.091998	0.092286	0.075124
Spec Heat @ T	BTU/(lb*R)	0.240085	0.240554	0.242562	0.242562	0.2599	0.310274	0.298625	0.298098	0.278856	0.278856	0.278856	0.240829	0.240829	0.240829
Spec Heat @ Ts	BTU/(lb*R)	0.239993	0.240289	0.242229	0.242188	0.259386	0.31022	0.29819	0.297304	0.278197	0.27782	0.275833	0.240479	0.240536	0.240115
Enthalpy @ T	BTU/lb	-4.31602	9.17643	47.9678	47.9678	203.173	717.219	515.175	509.678	287.035	287.035	287.035	14.9044	14.9044	14.9048
Enthalpy @ Ts	BTU/lb	-11.238	3.64356	44.1218	43.2676	198.949	715.861	508.259	497.048	281.001	277.865	261.317	7.60048	8.78896	-2.07971
Entropy Function @ T		-0.11924	0.240685	1.10766	1.10766	3.33061	6.92613	5.84201	5.80758	4.18686	4.18686	4.18686	0.382961	0.382961	0.382972
Entropy Function @ Ts		-0.319397	0.097556	1.03062	1.01328	3.2849	6.91971	5.80024	5.73042	4.13284	4.10445	3.95126	0.200508	0.23085	-0.056949
Exergy	BTU/lb	-0.357631	11.9472	51.0907	50.5625	200.308	584.854	384.247	379.623	147.506	146.508	146.508	17.6653	17.0043	17.0043
Gas Constant	BTU/(lb*R)	0.068607	0.068607	0.068607	0.068607	0.068607	0.068606	0.068606	0.068606	0.068606	0.068606	0.068606	0.068607	0.068607	0.068607
Fuel-Air-Ratio		0	0	0	0	0	0.028979	0.026318	0.025921	0.025792	0.025792	0.025792	0	0	0
Water-Air-Ratio		0	0	0	0	0	0	0	0	0	0	0	0	0	0

Figure 31: GasTurb14 detailed stations outputs at takeoff